JGR Atmospheres

RESEARCH ARTICLE
10.1029/2021JD036190

Effects of Lake Nam Co and Surrounding Terrain on Extreme Precipitation Over Nam Co Basin, Tibetan Plateau: A Case Study

Zhizhan Zhao[1,2], Anning Huang[1,2], Weiqiang Ma[3], Yang Wu[1,2], Lijuan Wen[4], Lazhu[5], and Chunlei Gu[1,2]

[1]CMA-NJU Joint Laboratory for Climate Prediction Studies, School of Atmospheric Sciences, Nanjing University, Nanjing, China, [2]State Key Laboratory of Severe Weather and Joint Center for Atmospheric Radar Research of CMA/NJU, School of Atmospheric Sciences, Nanjing University, Nanjing, China, [3]Key Laboratory of Tibetan Environment Changes and Land Surface Processes, Institute of Tibetan Plateau Research, Chinese Academy of Sciences, Beijing, China, [4]Key Laboratory of Land Surface Process and Climate Change in Cold and Arid Regions, Chinese Academy of Sciences, Lanzhou, China, [5]College of Science, Tibet University, Lhasa, China

Key Points:

- The extreme snowfall over Nam Co basin on 24 October 2006 cannot be reproduced without Lake Nam Co (LNC) and surrounding topography
- The hydrothermal effect of LNC plays a dominant role in the formation of the extreme snowfall event
- The terrain lifting effect on the westerlies from LNC further amplifies the lake effect snow over the downwind of the lake

Correspondence to:
A. Huang,
anhuang@nju.edu.cn

Citation:
Zhao, Z., Huang, A., Ma, W., Wu, Y., Wen, L., Lazhu, & Gu, C. (2022). Effects of Lake Nam Co and surrounding terrain on extreme precipitation over Nam Co basin, Tibetan Plateau: A case study. *Journal of Geophysical Research: Atmospheres*, *127*, e2021JD036190. https://doi.org/10.1029/2021JD036190

Received 12 NOV 2021
Accepted 4 MAY 2022

Author Contributions:
Conceptualization: Anning Huang
Data curation: Zhizhan Zhao, Yang Wu
Formal analysis: Zhizhan Zhao
Funding acquisition: Anning Huang
Investigation: Zhizhan Zhao, Anning Huang, Weiqiang Ma
Project Administration: Anning Huang
Supervision: Anning Huang
Validation: Zhizhan Zhao
Writing – original draft: Zhizhan Zhao, Anning Huang
Writing – review & editing: Anning Huang, Weiqiang Ma, Yang Wu, Lijuan Wen, Lazhu, Chunlei Gu

Abstract Thousands of lakes and complex topography on Tibetan Plateau (TP) have important impacts on the local weather and climate, especially extreme weather events. In this study, the Weather Research and Forecasting model was adopted to quantify the impacts of Lake Nam Co (LNC) and surrounding topography on the extreme snowfall event over Nam Co basin on 24 October 2006 based on numerical experiments. The accumulated precipitation of 12 hr in this event is characterized by a maximum precipitation center with an intensity exceeding 20 mm over eastern LNC and downwind regions. Results show that the precipitation regionally averaged over eastern LNC and downstream regions can be reduced by 53%, 26%, and 68% when LNC, surrounding terrain, and both of them are absent, respectively, suggesting that LNC plays a dominant role in the formation of this event while the surrounding mountains further amplify the lake effect precipitation/snow over the downwind of LNC. Mechanism analysis indicates that the low-level convective instability and water vapor convergence induced by LNC are essential for the formation of this extreme snowfall event, while the wind deflection and topographic lifting further strengthen the precipitation over the downwind of LNC and shift the snow belt distribution. This study is not only important to deepen the understanding of the complex interactions between the lake and orography and their combined influences on regional extreme precipitation, but also helpful for further improving the refined forecasting of the extreme precipitation induced by the lake and surrounding terrain in other regions over TP.

Plain Language Summary Lakes and complex terrain over Tibetan Plateau (TP), which is well known as "Asia's Water Tower" and "Roof of the World," play important roles in extreme weather events. To indicate the impacts of lakes and surrounding terrain over TP on extreme precipitation/snow, the Weather Research and Forecasting model, which can well reproduce the extreme snowfall event over Nam Co basin on 24 October 2006 in terms of intensity and distribution, is used to quantify the effects of Lake Nam Co (LNC) and surrounding topography on this event by a case study. We found that LNC played a dominant role in providing water vapor and energy for the formation of the extreme snowstorm while the lifting effect of Nyainqentanglha Mountains on the westerlies from the LNC further enhanced and redistributed the lake effect precipitation/snow over the downwind of LNC. This preliminary exploration deepens our understanding of the combined effects of lake and surrounding terrain on the extreme snowfall/precipitation under a certain atmospheric circulation background to some extent. Findings of this study can provide a base to further improve the refined prediction level of extreme snowfall/precipitation over lakes and surrounding areas on TP.

1. Introduction

Tibetan Plateau (TP), which is well known as the "Asia's Water Tower" and "Roof of the World," has the highest alpine lake concentrations in the world. And the sizes and numbers of these lakes have been experiencing rapid expansion over the past several decades (Dong et al., 2018; G. Zhang et al., 2021). Currently, TP harbors more than 1,400 lakes with an area of more than 1 km^2, including 13 lakes with an area of more than 500 km^2, and the total lake area exceeds 47,000 km^2 (Ma et al., 2009; F. Sun et al., 2020; Wan et al., 2014; Zhu et al., 2019). Lakes features with high specific heat capacity, low albedo, high clarity, low surface roughness, and high water vapor

supply, and plays distinct roles in modulating the land-air mass and flux exchange and surface energy balance compared with other land cover types (Bonan, 1995; MacKay et al., 2009; Su et al., 2020; B. Wang et al., 2020). As a result, the presence of large lakes would greatly alter the boundary layer condition and mesoscale circulations, and further affect the local weather and climate (Notaro, Holman, et al., 2013; Wen et al., 2015; Wu et al., 2019).

Lake climatic effects significantly vary with regions and timescales, that is, diurnal and seasonal. Previous studies of Great Lakes regions in North America have demonstrated that the water body can reduce the amplitude of the diurnal cycle and annual cycle of air temperature in the lake area, weaken the surface pressure (Notaro, Holman, et al., 2013), and trigger downwind snowfall during the cold season by high lake-air temperature difference which induce large heat release in terms of latent and sensible flux from the lake to overlying air (Eichenlaub, 1970; Kristovich et al., 2003; Miner & Fritsch, 1997; Niziol et al., 1995). The Great Lakes strongly increase precipitation over the downwind areas in winter and cause a relatively slight decrease over the lakes in summer (Notaro, Zarrin, et al., 2013; Scott & Huff, 1996). Kristovich and Spinar (2005) found an obvious morning maximum and afternoon/evening minimum in lake-effect precipitation frequency over the Great Lakes in winter. Studies for other temperate lakes (e.g., Lake Ladoga and Lake Taihu) have come to similar conclusions, which are closely related to lake-induced destabilization of the lower atmosphere and promotion of thermal convective activities (Gu et al., 2016; Samuelsson et al., 2010). As the largest group of freshwater bodies on the earth, the Great Lakes can produce more snowfall by the combined effects of lake clusters than by Lake Ontario alone (~200% more) and generally strengthen the cyclonic system near the surface in cold season (Lang et al., 2018; Xiao et al., 2018). However, tropical East African lakes show different climatic effects from temperate lakes (Van de Walle et al., 2020). Unlike the Great Lakes, low-latitude lakes have relatively higher temperatures than surrounding land and tend to increase precipitation in summer rainy season (Dutra et al., 2010). Because of the intense evaporation from water bodies (Gat & Matsui, 1991; Nicholson & Yin, 2002), tropical lakes lead to significant precipitation increases over the lake and adjacent areas due to continuous enhancements of water vapor mixing ratio, especially during nighttime (Diallo et al., 2018; Koseki & Mooney, 2019). In addition, the warm (cold) lake surface during nighttime (daytime) excites a large number of thunderstorms over Lake Victoria (surrounding land; Thiery et al., 2016).

Owing to the special features of TP, that is, high altitude, low air pressure, low air temperature, and intense solar radiation, strong lake-air interactions and lake effects shape the regional weather and climate (Ma et al., 2009; Wen et al., 2016; Wonsick & Pinker, 2014). However, the harsh environmental conditions cause great difficulty in meteorological observation (J. Sun et al., 2020; B. Wang et al., 2015). While benefiting from the development of regional climate models, scholars could simulate the lake-air interactions and lake effects with much finer resolution, compensating for the lack of observational data. Recent studies (Su et al., 2019; X. Yang et al., 2021; Zhu et al., 2018, 2020) suggested that due to heat transfer from the deeper part to the surface of the lake and the reduction in solar radiation absorption at upper-most water layer, lakes on TP tend to warm (cool) the surface atmosphere and enhance (weaken) the sensible and latent heat flux at nighttime (daytime) during autumn (summer). The heating and surface friction inconsistency between the lake and land produces obvious lake-land thermal and dynamic contrasts and excites the diurnal cycle in the lake-land breeze and vertical motions (L. Xu & Liu, 2015; L. Xu et al., 2014), which further causes the obvious diurnal cycle in convective precipitation over lakes (Su et al., 2020; Wen et al., 2015). Compared to low-latitude lakes, the hydrothermal effect on the stability of the air-lake boundary layer over the lakes on TP appears even stronger (Wen et al., 2016; Y. Xu et al., 2011). Similar to the temperate and boreal lakes, the lakes over TP show significant seasonal differences in their effects. Dai, Yao, et al. (2020) found that Lake Nam Co (LNC) can lead to a precipitation decrease of 45%–70% over the lake in summer but an increase of 60% over the lake and downwind areas in autumn. Similar conclusions were confirmed at Qinghai Lake on TP by Su et al. (2020). Although the thermal effect of lakes is suppressed in summer, X. Yao et al. (2021) indicated the surface friction contrasts between the water body and land can still enhance the precipitation over the downwind of Lake Selin Co on the central TP. Such a dynamic factor was also found to be effective in winter lake-effect precipitation (Behravesh et al., 2021). Wu et al. (2019) revealed that the climatic effects of lake clusters on TP are complicated by intrinsic lake features, local terrain, and background circulations. For example, large and deep lakes on the central TP tend to show strong heat effects and significantly enhance the convective rainfall during nighttime compared with small and shallow lakes on the north TP (Wu et al., 2019; Zhu et al., 2020).

Over the past decade, researchers have mostly focused on the climatic effects of lakes alone but few studies have paid attention to the comprehensive effects of TP lakes and surrounding terrain on local climate or extreme weather events. A recent study on the desiccated lake system in Mexico City has shown that the lake would climatologically enhance the intensity of heavy precipitation (López-Espinoza et al., 2019). Lake Victoria enhances the diurnal cycle in rainfall and significantly increases the frequency of extreme weathers, and the Gregory Ridge on the east side of Lake Victoria intensifies the convergence of the trade winds over the basin and triggers precipitation (Thiery et al., 2016; Van de Walle et al., 2020). During extreme events, the upstream and downstream topography can affect the amount and location of precipitation around the lakes (Alcott & Steenburgh, 2013; Hjelmfelt, 1992; Onton & Steenburgh, 2001). When lake surface temperature rises, the existence of orography further amplifies the precipitation intensity (Shestakova & Toropov, 2021). Umek and Gohm (2016) pointed out that the low-level boundary instability induced by the Lake Constance and orographic lifting are crucial for the formation of the snow belt. The analysis of the observed snowstorm in Lake Ontario has demonstrated that the orographic enhancement of precipitation promoted by the lake-induced instability and the land-breeze front along the Lake Ontario shoreline are the dominant contributors to the pronounced precipitation maximum over the Tug Hill (Campbell & Steenburgh, 2017; Veals et al., 2018). As one of the largest lakes on TP, the south and east sides of LNC are blocked by Nyainqentanglha Range with complex terrain around the lake basin (Figure 2b). Since the 21st century, the observations and numerical simulations of lake-air interactions in Nam Co basin have been gradually developed (Biermann et al., 2013; Li et al., 2009; Maussion et al., 2010; B. Wang et al., 2015). Gerken et al. (2013) used a two-dimensional ideal model to simulate the lake breeze in the Nam Co basin, then proposed two possible circulation mechanisms for convection triggering. X. Yang et al. (2015) found that LNC together with Nyainqentanglha Mountains may strengthen the mesoscale circulation around the lake in summer. Previous studies have given the seasonal and spatial distribution characteristics of precipitation over the Nam Co basin (Dai, Yao, et al., 2018; J. Xu et al., 2018). A 1-month simulation carried out in October 2006 showed that LNC caused more than 70% downwind precipitation during the extreme snowfall event on 24 October 2006 (Dai, Wang, et al., 2018). Dai, Chen, et al. (2020) further conducted a simulation along 31°–32°N in the southern part of TP and indicated that the monthly snow depths over the downwind area of LNC were much deeper than other large lakes over TP. The in-situ observed frequency and intensity of extreme snowfall (precipitation) events also showed significant increasing trends during the past 15 years over the Nam Co basin (Dai, Chen, et al., 2020). The extreme precipitation expands the risk of mountain hazards in alpine region and poses a severe challenge to the fragile ecological environment (Cui & Jia, 2015; Gao et al., 2018; Ge et al., 2017; Ma et al., 2018; L. Wang et al., 2017).

Previous studies suggested that the long east-west axis of LNC, as well as the barrier of Nyainqentanglha Mountains, may contribute to the stronger lake-effect snowfall compared with other large lakes such as Lake Selin Co (Dai, Chen, et al., 2020; Kropacek et al., 2010). However, it is unclear how much the LNC together with the surrounding topography contributes to the extreme precipitation and what the underlying physical mechanisms are. To address these issues, in this study we used the Weather Research and Forecasting (WRF) model to reproduce the extreme snowfall event on 24 October 2006 over Nam Co basin (Dai, Wang, et al., 2018) and quantify the relative contribution of the LNC and surrounding topography through a set of sensitive experiments. Meanwhile, the underlying physical mechanisms related to the formation of the extreme snowfall induced by LNC and surrounding terrain will be further explored. Findings of this study may deepen our understanding of the combined effect of alpine lakes with surrounding terrain and provide a reference to further improve the refined forecasting of extreme precipitation/snowfall events over lakes and adjacent areas on TP.

2. Study Area, Data, Numerical Experimental Design

2.1. Study Area

During 00:00–12:00 local solar time (LST) on 24 October 2006, an extreme precipitation event occurred over the mid-east part of LNC and the adjacent downwind areas. It was the fourth-strongest extreme precipitation event in cold season during 2005–2016 with the accumulated precipitation of 14.1 mm observed at Nam Co station (Dai, Wang, et al., 2018). The China Meteorological Forcing Data Set (CMFD; He et al., 2020; K. Yang & He, 2019, available at http://data.tpdc.ac.cn) also captured this extreme precipitation (Figures 1d–1f), it is shown that the precipitation center moved southeastward across the eastern LNC. The concomitant atmospheric circulations (Figures 1a–1c) was featured by a low vortex at 500 hPa level moving southeastward during midnight to

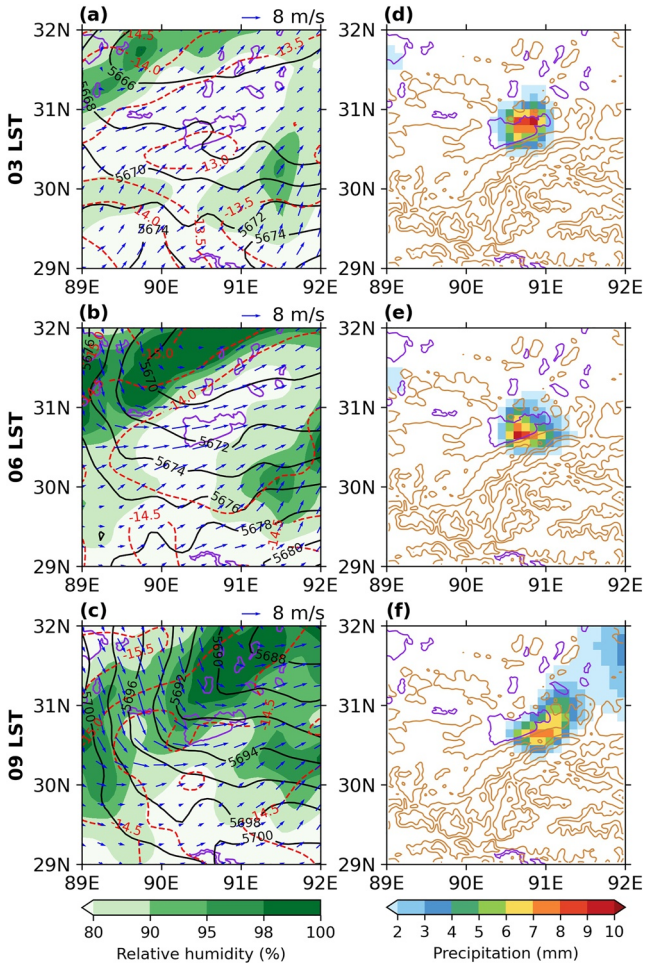

Figure 1. Geopotential height (gpm, black solid lines), temperature (°C, red dashed lines), relative humidity (%, shaded), and wind vector at 500 hPa from ERA5 at (a) 03:00 LST, (b) 06:00 LST, and (c) 09:00 LST on 24 October 2006. (d–f) Three-hour accumulated precipitation of China Meteorological Forcing Data Set is shown for the corresponding moment (purple and yellow contour lines identify the boundary of lakes and terrain height, respectively).

morning and sufficient water vapor transport with the relative humidity over 90% over most areas of Nam Co basin. The wind field at 500 hPa transformed from a strong southwesterly wind to a strong northwesterly wind over the LNC, accompanied by the wind shear and cold advection to the lake area. Such a circulation condition provided favorable large-scale environmental conditions for the occurrence of this extreme snowfall event (Alcott & Steenburgh, 2013).

To address how LNC and the surrounding orography affect this extreme snowfall and the underlying mechanisms, we focus on the Nam Co basin and surrounding areas indicated by the red box in Figure 2a, where the topography and land cover types are diverse (Figures 2b and 2c). In addition to wetland and lake land types, such as LNC which is the second largest lake on the central TP (30°30′−30°56′, 90°16′−91°03′, Figure 2) with an area of more than 2,000 km^2, the mean depth of 40 m and altitude of 4,718 m (Lazhu et al., 2016; J. Wang et al., 2009; Wu & Zhu, 2008) and begins to freeze in mid-January and completely melts by the end of April with an average ice period of about 87 days (Gou et al., 2017), there are sparse shrubs, grasslands, hills, and mountains covered by glaciers and snow over Nam Co basin. The Nyainqentanglha Mountain extending from southwest to northeast is located along the south and east sides of LNC with a mean altitude of ~6,000 m. The entire mountain range contains approximately 6,426 glaciers (Ji et al., 2018). For simplicity and convenience, the Nyainqentanglha Mountain (NQTL) is divided into three parts: west NQTL, central NQTL, and east NQTL (Figure 2b). The Nam Co basin is affected by the southwest monsoon in the warm and wet season while controlled by westerly circulation in the cold and dry season (T. Yao et al., 2013).

2.2. Data

The data used in current study are listed as follows:

1. The fifth-generation ECMWF atmospheric reanalysis (ERA5), which is the latest generation to replace its predecessor ERA-Interim reanalysis, provides global atmospheric and land surface information, including 37-level air pressure, temperature, humidity, and winds with a horizontal resolution of 0.25° × 0.25° and land surface data with a horizontal resolution of 0.1° × 0.1° at the temporal resolution of 3 hr from 1950 to the present (Hersbach et al., 2020). It is available at the website https://www.ecmwf.int/en/forecasts/datasets/search/ERA5.
2. The CMFD with a temporal resolution of 3 hr and a spatial resolution of 0.1° from 1979 (currently up to 2018; He et al., 2020; K. Yang & He, 2019, available at http://data.tpdc.ac.cn) is derived from a fusion of remote sensing products (GEWEX-SRB and TRMM), reanalysis data set, and CMA in-situ observation data. It is one of the most widely used data sets in China. CMFD provides 7 near-surface meteorological elements, including surface pressure, 2 m air temperature and specific humidity, 10 m wind speed, downward shortwave radiation, downward longwave radiation, and precipitation rate. In this study, we used the precipitation data of CMFD to analyze the temporal evolution of snowfall and evaluate the amount and distribution of simulated precipitation.
3. The meteorological observation data from the integrated observation at the research stations of multiple spheres in Nam Co basin, including the daily temperature, air pressure, relative humidity, wind speed, precipitation, and radiation observed at Nam Co station (30°45′N,90°56′E, marked with a red triangle in Figure 2) from 1 October 2005 to 31 December 2016, was used to validate the reliability of simulated precipitation supplementally. After eliminating systematic errors caused by missing data points and sensor failures, the data set achieved the accuracy of raw meteorological observation data required by the China National Weather

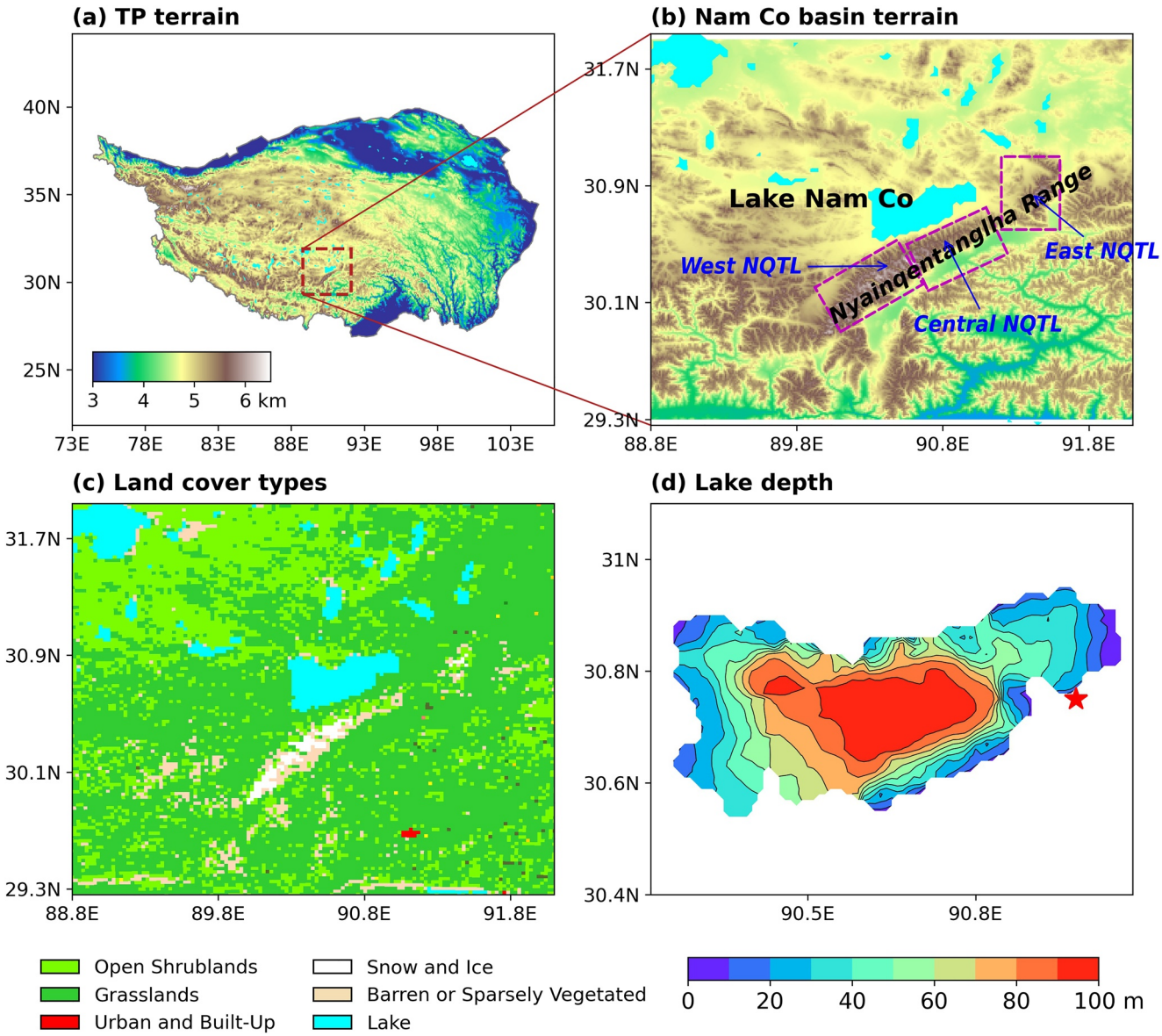

Figure 2. (a) Terrain height of Tibetan Plateau and the location of Lake Nam Co (LNC); (b) terrain height of Nam Co basin, and the purple boxes divide Nyainqentanglha Range into three parts (west, central, and east NQTL); (c) land cover types of Nam Co basin; (d) bathymetry of LNC (unit: m, red asterisk mark indicates the Nam Co observational station).

Service and the World Meteorological Organization (WMO; Y. Wang & Wu, 2018). More detailed information can be found at http://data.tpdc.ac.cn.

4. The Terra satellite platform with the Medium Resolution Imaging Spectroscopy (MODIS) instrument transits at 10:30 a.m. and 10:30 p.m. LST to generate the twice-daily 1 km resolution land surface temperature and emissivity data product MOD11A1. The detailed introduction can be found at https://modis.gsfc.nasa.gov/data/dataprod/mod11.php.
5. The IGBP modified MODIS land-use categories with a resolution of 10 arc seconds (Friedl et al., 2010), which is available at https://lpdaac.usgs.gov/products/mcd12q1v006/, and the global lake database version 2 (GLDBv2) including the lake location and depth with the horizontal resolution of 1 km (Choulga et al., 2014; Kourzeneva, 2010) is available at http://www.flake.igb-berlin.de/site/external-dataset.

2.3. Model Configuration and Numerical Experimental Design

The WRF Model version 3.9.1 coupled with a 1-D lake model (Wu et al., 2020) is used in the current study. It is designed by National Center for Atmospheric Research for atmospheric research and operational forecasting applications (Powers et al., 2017). The lake component scheme in WRF is a 1-D mass and energy balance model (Gu et al., 2015) with up to 5 snow layers on the lake ice, 25 lake water/ice layers, and 10 soil layers in the bottom sediment (Subin et al., 2012). This lake model with some key parameters tuned can well reproduce the variation of the lake surface temperature and the thermal stratification of LNC (Huang et al., 2019; Wu et al., 2020). Compared to the WRF model uncoupled with the 1-D lake model, the lake-air coupled model can significantly improve the simulation of meteorological elements such as precipitation and temperature over the lake and surrounding areas (Gu et al., 2016; Ma et al., 2019; F. Wang et al., 2019; Wu et al., 2020). Numerical simulations for LNC have shown that increasing the lake eddy diffusion coefficient can mitigate the rapid cooling due to insufficient mixing of highland lakes in autumn (Fang et al., 2017; Huang et al., 2019). A series of experimental results have proven that increasing the lake eddy diffusion coefficient, decreasing the extinction coefficient and the maximum water density temperature, as well as adopting a parameterized surface roughness length can effectively reduce the overestimation of 2 m air temperature over the lake and downwind precipitation (Wu et al., 2020; Xiao et al., 2016; L. Xu et al., 2016). In this study, the key parameters in the lake component model were set as the same as in the study of Wu et al. (2020), who calibrated the lake component model in WRF3.9.1 well. In addition, the main physical parameterization schemes adopted in this study are listed as follows: WRF single–moment 6-class microphysical scheme (Hong & Lim, 2006); Grell–Devenyi ensemble cumulus scheme (Grell & Dévényi, 2002); RRTM longwave radiation scheme (Mlawer et al., 1997); Dudhia shortwave radiation scheme (Dudhia, 1989); Noah land surface scheme (Tewari et al., 2004); and YSU planetary boundary layer (Hong et al., 2006).

The horizontal resolution of 5 km and 40 sigma vertical levels of atmosphere were applied for the WRF simulation over the study region including LNC and the neighboring areas (Figure 2b). The model domain was centered at (30.45°N, 90.60°E) with 72 × 54 grid points and the time step was set to 30 s. The land surface types at each WRF model grid were derived from the MODIS land-use categories (Friedl et al., 2010). The lake fraction (sub-grid lake area/grid area) and depth at each WRF model grid were derived from the GLDBv2 lake location and depth data. As the depth of LNC is very unreal in the GLDBv2 data set, it was updated by the observed lake depth (Figure 2d from J. Wang et al. [2009]). Meanwhile, the lake temperature initialization has a significant impact on model results (Mallard et al., 2014, 2015; X. Zhang et al., 2016). According to previous studies, the whole water body of LNC is uniformly mixed and water temperature from top to bottom exhibits very small differences at the end of October (Huang et al., 2019). Following Wu et al. (2020), the lake water temperatures at all vertical layers were initialized by the MODIS lake surface temperature.

In this study, we set up 4 experiments namely CTL, EXP_NL, EXP_NM, and EXP_NLM with the CTL as the control experiment and the others as sensitivity experiments: the CTL experiment adopted default setting including the LNC and its surrounding orography (Figures 3a and 3e); the LNC was replaced by the adjacent land cover types in the EXP_NL experiment (Figures 3b and 3f); the terrain height of the neighboring area above the elevation of LNC (4,817 m) was set to 4,817 m in the EXP_NM experiment (Figure 3g), and the snow and ice on the Nyainqentanglha Mountains were recovered by the adjacent land cover types (grassland, Figure 3c); LNC and its surrounding orography were replaced by the nearby land cover types in the EXP_NLM experiment (Figures 3d and 3h). All experiments shared the same model configurations and were driven by the same initial and lateral boundary conditions of atmosphere, which were derived from the 3-hourly ERA5 data. Each experiment started from 00:00 UTC on 23rd October and ended at 00:00 UTC on 25 October 2006 with the first 12 hr for model spin-up.

3. Results

3.1. Model Validation

To indicate the performance of the WRF model in reproducing the extreme snowfall event over Nam Co basin on 24 October 2006, Figure 4 gives the spatial distribution of accumulated precipitation from CMFD and CTL simulation during 00:00–12:00 LST on 24 October 2006. It can be noted that the WRF model can reasonably reproduce the intensity and spatial pattern of precipitation with a spatial correlation coefficient of 0.54 (at 0.01

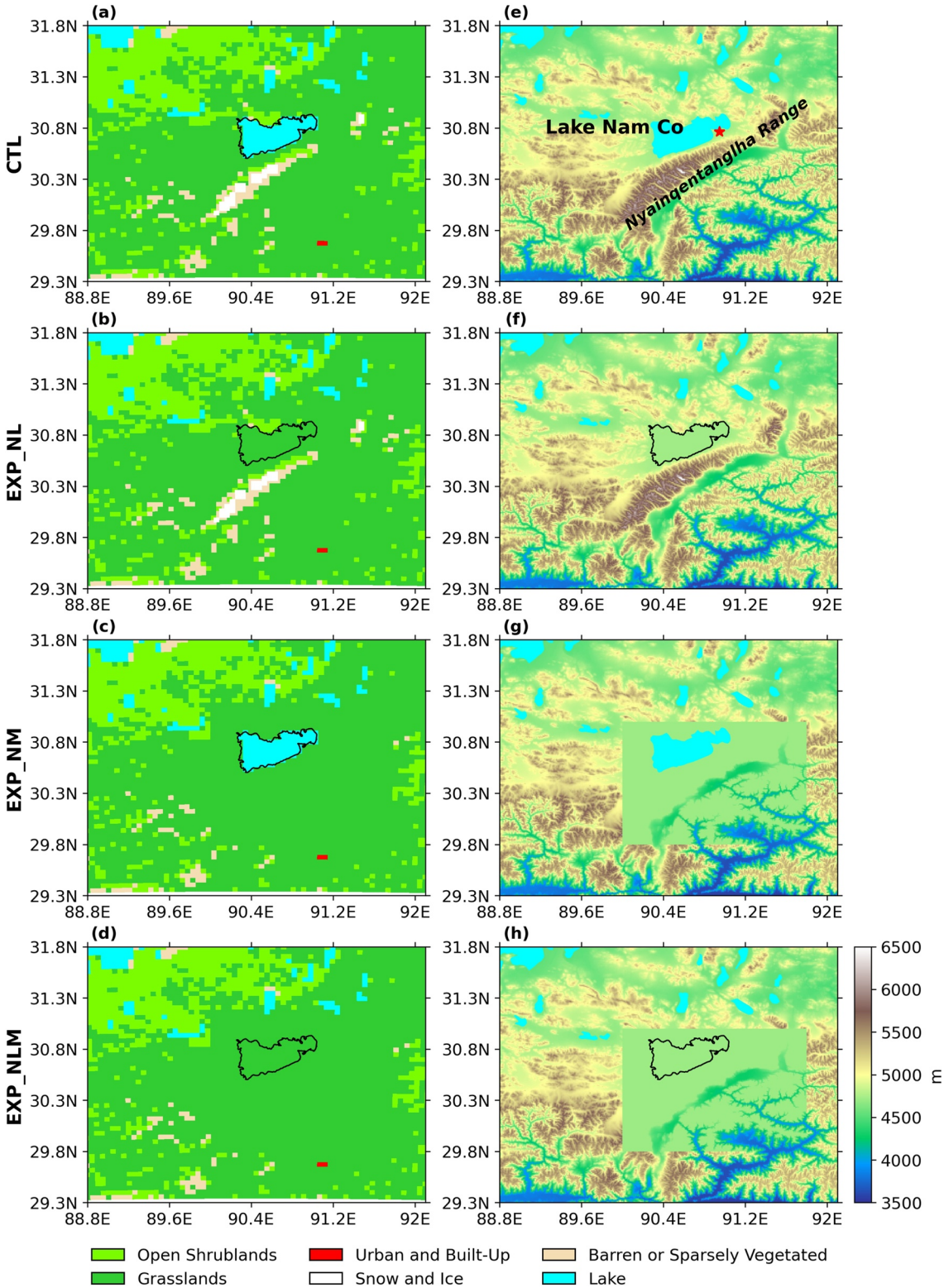

Figure 3. (a–d) Terrain height and (e–h) land cover types in each experiment.

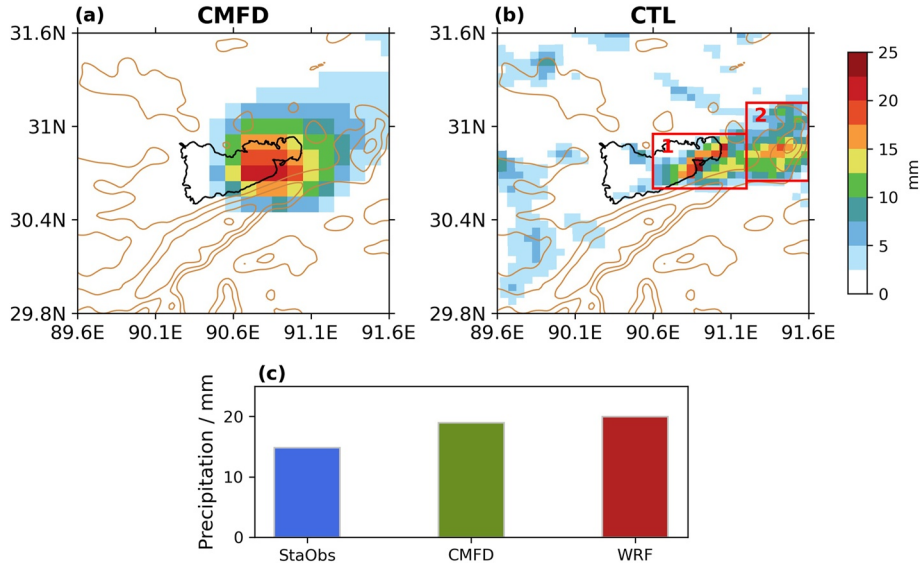

Figure 4. (a) Spatial distribution of the China Meteorological Forcing Data Set (CMFD) observed and (b) CTL modeled accumulated precipitation during 00:00–12:00 LST on 24 October 2006. (c) Comparison of the CTL simulation against the accumulated precipitation from the Nam Co station and CMFD observation during the precipitation extreme event on 24 October 2006. The CTL simulation and CMFD data were interpolated onto the observation station by bi-linear interpolation. Contours show the terrain height.

significance level) over the entire simulation domain (Figures 4a and 4b), despite that the intensity of precipitation along the east shore of the lake is slightly overestimated and the modeled extent of snowfall center over eastern LNC is smaller than the observation. The simulated snowfall belt is located along the east shore of LNC and the windward slope of east NQTL in the downwind direction with intensities exceeding 25 and 15 mm, respectively (Figure 4b), which is closely associated with the direction of the prevailing wind over the land surface and the forcing of the complex terrain around LNC.

Figure 4c gives the comparison of CMFD observed and WRF simulated precipitation at the location of Nam Co station (30°45′N, 90°56′E) against the in-situ observation to further verify the accuracy of modeled precipitation. The precipitation amount simulated by WRF is slightly higher than the observation. As Nam Co station is located at the junction of the lake and mountains with complex surrounding underlying surface conditions, and the model results with a resolution of 5 km deviate from the location of the Nam Co station, which seems to cause the model bias. Combined with the spatial distribution of precipitation from CMFD, the model results are comparable with observations. Overall, the WRF model can reasonably reproduce this extreme snowfall event in terms of intensity and spatial distribution. It can be used to study the effects of LNC and its surrounding terrain on the occurrence of this extreme snowfall event.

3.2. Impacts of LNC and Surrounding Terrain on the Extreme Snowfall on 24 October 2006

This section will demonstrate how the LNC and its surrounding terrain affect the extreme snowfall on 24 October 2006 and their relative importance. Figure 5 gives the spatial distribution of accumulated total precipitation during the extreme snowfall event from three sensitive experiments and the simulated precipitation differences (including total precipitation, convective precipitation, and large-scale precipitation) between each sensitive experiment and the CTL experiment. To facilitate the quantification, Table 1 lists the regional mean precipitation simulated by each experiment in two sub-regions (sub-reg1 containing the lake and the part of the downwind land and sub-reg2 containing the downstream orography, Figure 4b).

From Figure 5a, the strong precipitation center over eastern LNC and lake shore regions in the CMFD observation (Figure 4a) and CTL simulation (Figure 4b) is absent in the EXP_NL experiment when the water surface type in the area of LNC is replaced by nearby grass type (i.e., no lake grid included). Although the precipitation center with the intensity of ∼10 mm along the slope of east NQTL in the sub-reg2 is still reproduced, the mean

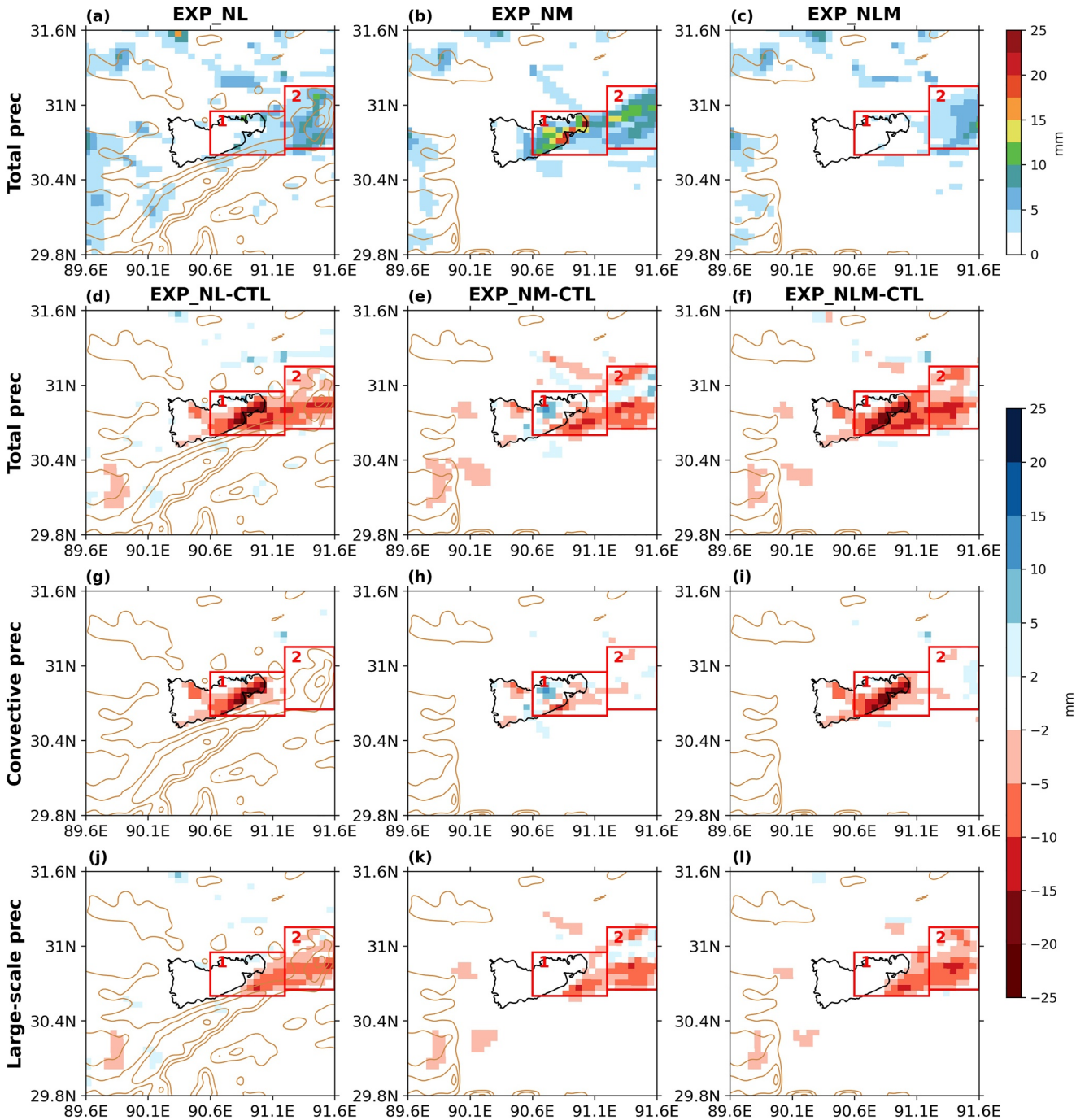

Figure 5. Spatial distribution of the accumulated total precipitation from 00:00 to 12:00 LST on 24 October 2006 produced by sensitive experiments (a–c) and their differences from the CTL experiment (d–f). Same as Figures 5d–5f, but for the differences in convective precipitation (g–i) and large-scale precipitation (j–l). Contours show the terrain height.

precipitation amount is largely decreased by 40% relative to the CTL experiment simulation (Figure 5a and Table 1). The significant reduction of simulated convective and large-scale precipitation occurs over the lake and the downwind areas, respectively, indicating that LNC as the hydrothermal source and adjacent topography is the influencing factors for both types of precipitation (Figures 5g and 5j). The modeled regional mean convective precipitation over sub-reg1 is reduced by 73% due to the absence of LNC relative to the CTL simulation (Table 1).

Table 1
Simulated Precipitation During 00:00–12:00 LST on 24 October 2006 for Sub-Reg1, Sub-Reg2 and the Entire Domain Shown in Figure 4

	Mean convective precipitation (mm)		Mean large-scale precipitation (mm)		Mean total precipitation (mm)		
Experiment	Sub-reg1	Sub-reg2	Sub-reg1	Sub-reg2	Sub-reg1	Sub-reg2	Entire domain
CTL	6.3	2.1	2.6	6.7	8.9	8.8	8.8
EXP_NL	1.7	1.8	1.0	3.4	2.7	5.2	4.1
EXP_NM	6.0	1.9	1.2	4.0	7.2	5.9	6.5
EXP_NLM	0.9	2.0	0.3	2.2	1.2	4.2	2.8

The difference in total precipitation between the EXP_NL and CTL simulation (Figure 5d) is consistent with the results of Dai, Yao, et al. (2018).

Relative to the CTL experiment simulation (Figure 4b), the EXP_NM experiment with lake surface but without the surrounding mountains still reproduced the strong precipitation center over eastern LNC and lake shore regions (Figure 5b), but the precipitation along the regions from the southeast shore of LNC to the north slopes of central NQTL was reduced by 5–15 mm (Figure 5e). However, the precipitation center with an intensity of ~12.5 mm over the sub-reg2 in Figure 4b was primarily reproduced (Figure 5b) but with an underestimation of ~5 mm (Figure 5e). The absence of the LNC surrounding orography mainly leads to the reduction of large-scale precipitation regionally averaged over the sub-reg1 (sub-reg2) by about 54% (40%; Table 1) and further affects the extent of the precipitation center.

The EXP_NLM experiment without LNC and its surrounding terrain failed to reproduce the precipitation centers in CMFD observation and CTL simulation despite a weak precipitation center simulated in the eastern sub-reg2 (Figure 5c). The precipitation amount during the extreme snowfall event was dramatically inhibited (Figure 5f) due to the absence of LNC and its surrounding terrain, which lead to the regional mean precipitation in sub-reg1, sub-reg2, and the entire domain (sub-regs 1 and 2) being reduced by 86%, 52%, and 68%, respectively (Table 1). Contrary to the expected result, the terrain and land cover that underwent substantial modification have not completely suppressed the precipitation on the downwind land of the eastern shore of LNC, where the amount of maximum precipitation is 9.8 mm.

Generally, the accumulated precipitation amount in each sensitive experiment was weakened to different degrees relative to the CTL experiment in the extreme snowfall event due to the absence of LNC, surrounding terrain, or both. Overall, the presence of LNC determined the intensity and location of this extreme snowfall event to a considerable degree, while the surrounding terrain such as NQTL can lead to strengthened precipitation along the regions from the southeast shore of LNC to the north slopes of central NQTL and the downwind land of LNC to the southern slope of east NQTL and further expand the extent of snowfall belt. The statistics in Table 1 indicate that the influences of the lake and topography on precipitation cannot be simply linearly summed. There are still other factors in addition to land-atmosphere interaction that affect the amount and distribution of precipitation. The influential mechanisms of multiple factors and their synergistic effects on the occurrence of this extreme snowstorm will be analyzed in the following section.

3.3. Possible Mechanisms

From the above analysis in Section 3.2, we have obtained the information about the impacts of LNC and its surrounding terrain on the extreme snowstorm on 24 October 2006, but the underlying physical mechanisms were not revealed and addressed.

Previous studies (Shi & Xue, 2019; Umek & Gohm, 2016) have suggested that the temperature difference between the lake surface and the overlying atmosphere is a key factor for the formation of lake-effect rainfall/snowfall. Before LNC freezing, the lake-air temperature difference reaches a peak (Du et al., 2020). In this event, the daily mean temperature difference between the lake surface and 500 hPa arrived at 19.5°C, which provides the

thermodynamic prerequisite for lake-effect snowfall. Surface processes associated with high lake-air temperature differences, such as heat flux and water vapor transport, deserve to be investigated primarily (Lazhu et al., 2016).

To illustrate how the lake and surrounding mountains affect this extreme snowstorm and through what key physical processes, Figure 6 first gives the spatial distribution of the differences in surface-2 m temperature difference, 10 m wind speed, 2 m air specific humidity, surface latent and sensible heat fluxes simulated by each sensitive experiment from the CTL simulations averaged over 03:00–09:00 LST on 24 October 2006. Replacing the water body type of LNC with grass type tends to result in the temperature difference between surface and 2 m air dramatically reduced by 6–10°C (Figures 6a and 6c), the 10 m wind speeds slowed down by 2–4 ms^{-1} (Figures 6d and 6f), the near-surface air specific humidity attenuated by 0.4–1.2 gkg^{-1} (Figures 6g and 6i), the latent heat flux significantly decreased by 80–160 Wm^{-2} (Figures 6j and 6l) and the sensible heat flux obviously weakened by 40–80 Wm^{-2} (Figures 6m and 6o) over the LNC area compared to the CTL simulations, suggesting that LNC played an important role in heating and moistening the lower atmosphere which provided favorable thermal and water vapor conditions for the formation of this extreme snowstorm. When the cold air moves across LNC with much warmer and moister surface, the strong lake-air temperature difference leads to intense instability of lower atmosphere, which favors triggering convection and thereafter precipitation significantly increases over downwind regions (Figures 6j and 6l).

Removing the surrounding mountains of LNC mainly results in the near-surface air specific humidity increasing by up to 1.2 gkg^{-1} due to the reduction in altitude over the mountainous areas flattened in the EXP_NM and EXP_NLM experiments (Figures 6h and 6i). The absence of the surrounding terrain tends to decrease the surface wind speeds around the lake area, especially along the north slope of west NQTL removed in EXP_NM to the east shore of LNC (Figure 6e), which further slightly increases the temperature difference between surface and 2 m air but reduces the 2 m air specific humidity, latent and sensible heat fluxes over LNC (Figures 6h, 6k, and 6n).

Figure 7 further displays the impact of LNC and surrounding terrain on the circulation in the atmospheric boundary layer. From Figure 7a, the northwest wind from north and southwest wind along the west NQTL merge over the western part of LNC and change to prevailing westerlies along the lake. Meanwhile, a strong convergence center can be noted in eastern LNC and near coastal areas. From Figures 7e and 7g, the removal of LNC leads to obviously weakened wind speeds over the lake due to the strengthened surface friction, and thereafter the convergence is obviously reduced over the eastern part of LNC and downwind areas. It is also noted that the convergence along the north side of central NQTL is significantly weakened due to the absence of terrain blocking, downhill wind from west NQTL, and lifting for the westerlies moving from LNC (see the red box in Figure 7f). Without the interference of complex terrain, the southerly wind near Dangxiong County located at the southeastern foot of the central NQTL can intersect with the westerly wind to the north (see red boxes in Figures 7c and 7d), creating a narrow low-level jet zone over the downstream of LNC which further results in the precipitation center along the northwest slope of east NQTL (Figures 5b and 5c). Benefiting from the complimentary water vapor transport from the lake, the precipitation amount over the downstream of LNC simulated by EXP_NM is much higher than that simulated by EXP_NLM (Figures 5b and 5c) in spite of similar wind field patterns (Figures 7c and 7d).

Overall, the extreme snowstorm cannot be reproduced without the thermal effect of LNC (Figures 5a, 6d, 6j, and 6m) or the dynamic impact of NQTL (Figures 7f and 7g), which favors the formation of convergence in the atmospheric boundary layer over the precipitation center. Another possible reason for the formation of the convergence zone is that the land breeze circulation induced by the thermal contrast between lake and land weakens the wind speed from lake to land (Gerken et al., 2013). In addition, the long east-west distance of LNC also gives the dry and cold air masses sufficient time to absorb water vapor and energy, and finally triggers convective storms before they leave the heat and water vapor source (Alcott & Steenburgh, 2013; Onton & Steenburgh, 2001; Umek & Gohm, 2016).

As shown in Figure 8a, extremely large vertical equivalent potential temperature gradients appear over LNC. During the extreme snowstorm, LNC with a much warmer surface relative to surrounding land constantly provides sufficient latent and sensible heat to create a warm and moisture pool and strong convective instability ($\partial\theta_e/\partial z < 0$) within 300 m above the lake, which alters the structure of the planetary boundary layer and continuously supplies water vapor and energy for the convective storms. The convergence at the land-lake junction together with the topographic uplifting along the downstream windward slope results in the intensive vertical upward motion extending from the boundary layer to the level of 7,000 m over the wide range of the eastern

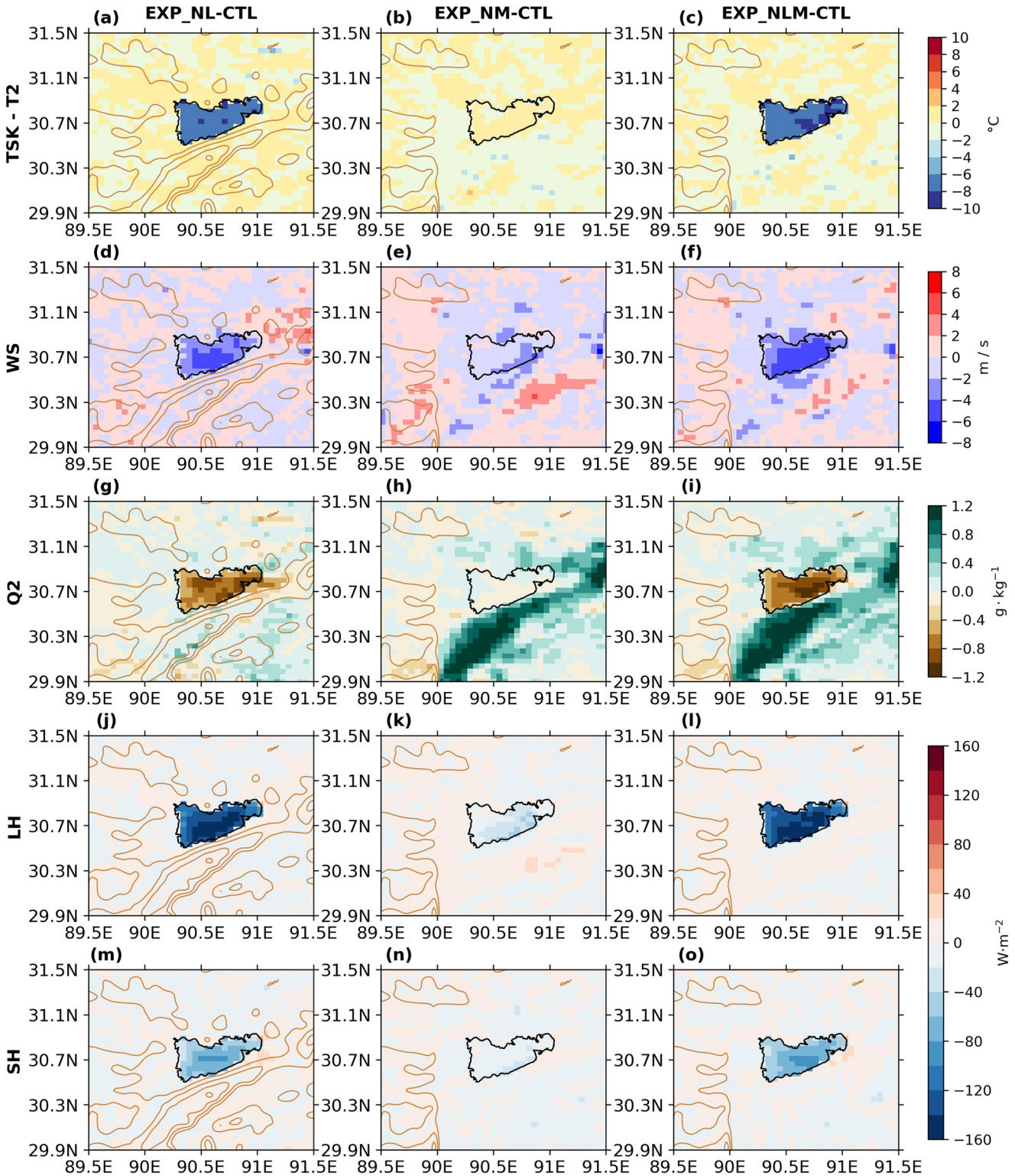

Figure 6. Spatial distribution of the differences in surface-2 m temperature difference, 10 m wind speed, 2 m air specific humidity, surface latent and sensible heat fluxes simulated by each sensitive experiment from the CTL simulations averaged over 03:00–09:00 LST on 24 October 2006. Contours show the terrain height.

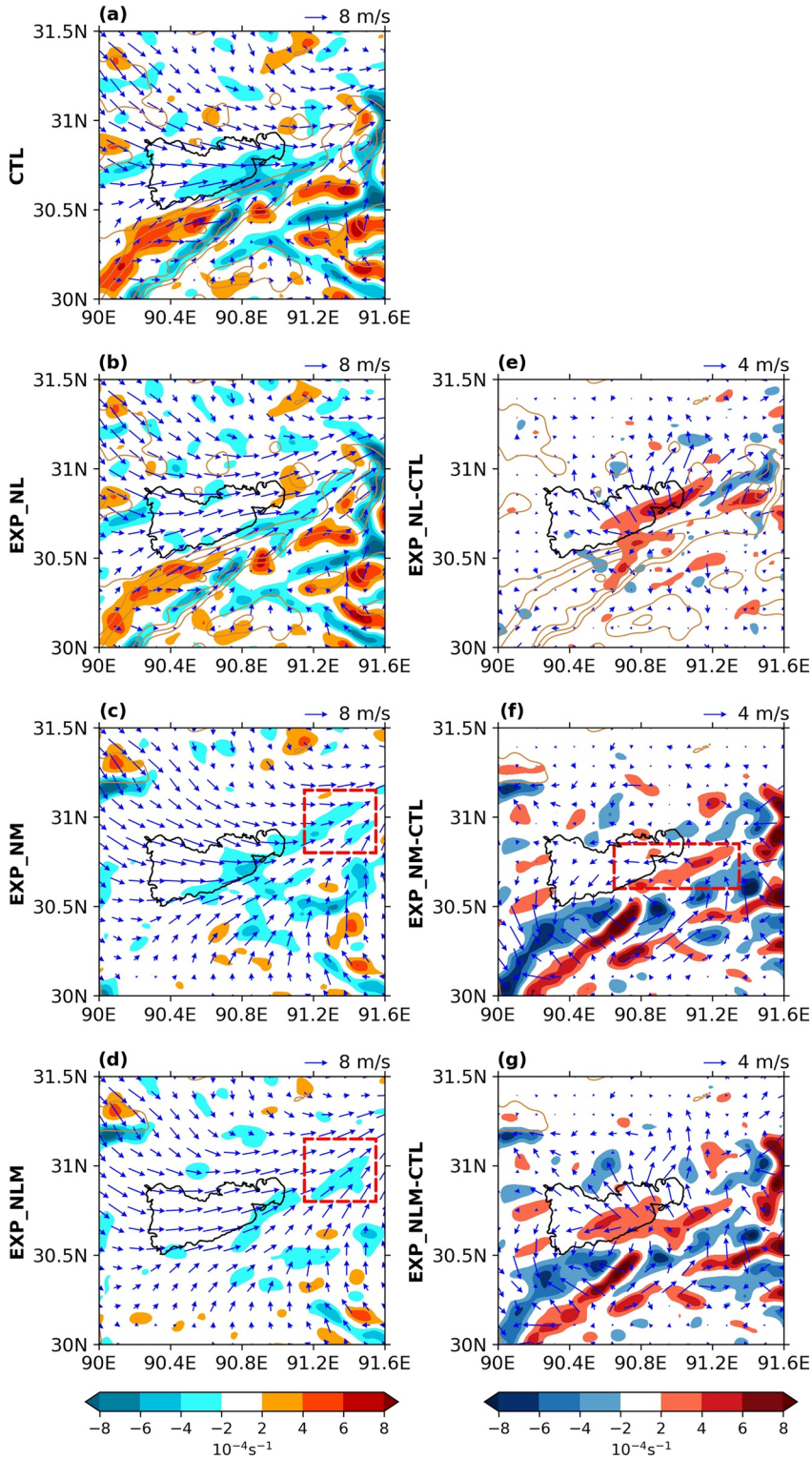

Figure 7. Spatial distribution of the simulated wind vector and divergences (shaded) at 150 m above ground level and their differences between each sensitive experiment and CTL experiment averaged over 03:00–09:00 LST on 24 October 2006. Contours show the terrain height.

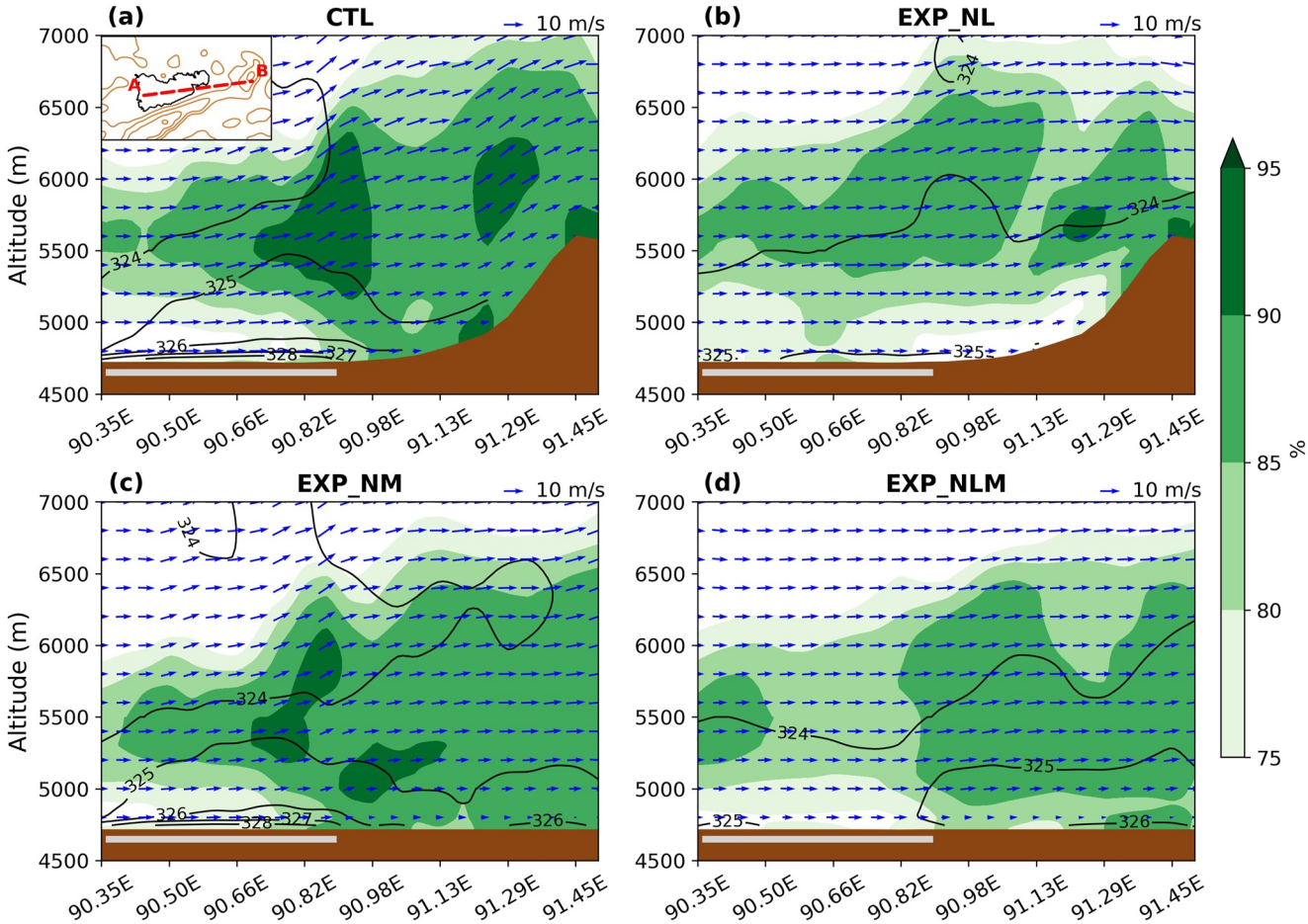

Figure 8. The vertical cross section of the modeled relative humidity (units: %, shaded), equivalent potential temperature (units: K, contours) and longitudinal circulation (vector, the vertical velocity was enlarged by 10 times) along the A–B red line in the inset of (a) averaged over 03:00–09:00 LST on 24 October 2006. The gray thick solid lines denote the location of Lake Nam Co and the brown shadings indicate the model topography in each experiment.

LNC and downwind areas, which further leads to large precipitation centers over eastern LNC and downstream (Figure 4b). The EXP_NL experiment without considering the impact of LNC fails to reproduce the low-level convective instability layer over the lake (Figure 8b) due to the much drier and colder lower atmosphere compared to the CTL simulation (Figure 9a) and thereafter the precipitation center in the eastern LNC and near lake shore areas (Figures 4b and 5a). The topographic uplifting of the prevailing westerlies at most layers below 7,000 m led to the vertical upward motions in the lower atmosphere along the windward slope of the east NQTL (Figure 8b) where the precipitation center can be partially simulated despite the underestimated intensity (Figures 5a and 5d), which is resulted from the dry subsidence zone over the east NQTL due to the significantly weakened upward motion over upstream LNC relative to the CTL simulation (Figure 9a).

The scope of upward motions induced by LNC simulated by the EXP_NM experiment without the downstream topography but the LNC included is mainly confined over the eastern LNC (Figure 8c), which corresponds well to the convergence zone and precipitation center over the lake (Figures 5b and 7c). Meanwhile, the existence of LNC can moisten and heat the dry and cold air moving across the much warmer lake surface, the moistened air with sufficient water vapor can be transported by the westerlies to the downstream areas, so the precipitation center over east NQTL can be reproduced to some extent (Figures 5b and 7c). However, compared to the CTL simulations, the EXP_NM experiment without the NQTL blocking and merging effects produces slightly weakened sensible and latent heat from LNC to the overlying atmosphere (Figures 6e, 6h, 6k, and 6n), which further leads to the relatively drier and colder atmosphere over LNC with an anomalous subsidence zone over the east LNC and near lake shore areas (Figures 7f and 9b). In addition, the absence of NQTL uplifting leads to a strong anomalous subsidence zone and thereafter significantly decreased precipitation over the mountainous areas south

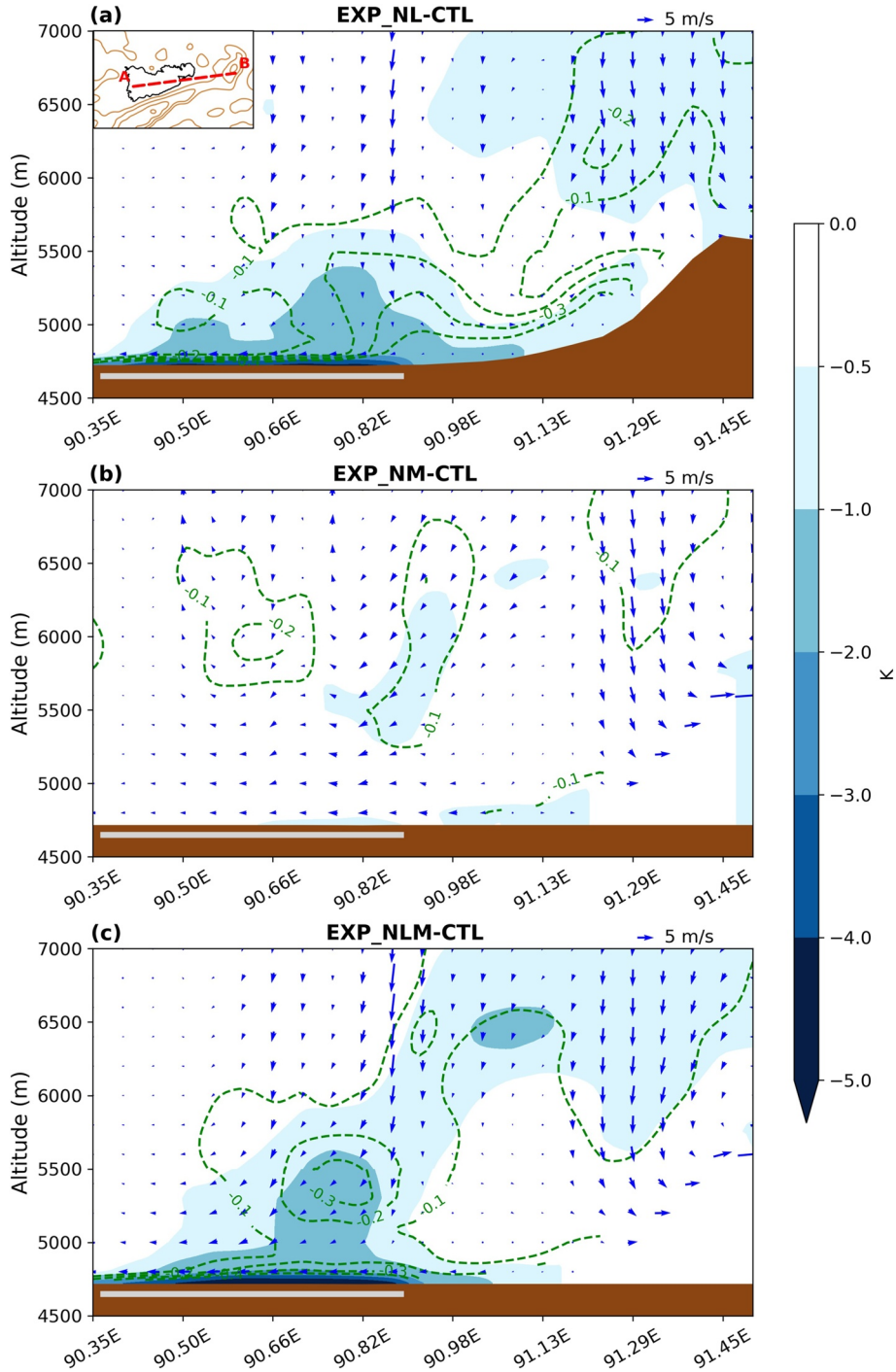

Figure 9. Same as Figure 8, but for the differences in the specific humidity (green contour lines, units: gkg^{-1}), equivalent potential temperature (shading) and longitudinal circulation (vector, the vertical velocity was enlarged by 10 times) simulated by each sensitive experiment from the simulation of CTL experiment.

of the precipitation belt (Figure 5e). Compared to the CTL simulations (Figure 8a), the EXP_NLM experiment without the LNC and NQTL produces prevailing westerlies (Figure 8d) with much colder and drier anomalies extending from the atmospheric boundary layer to the altitude of 6,000 m over LNC and anomalous subsidence motions over east NQTL (Figure 9c), leading to the failed simulation of the extreme snowstorm center (Figures 5e and 5f).

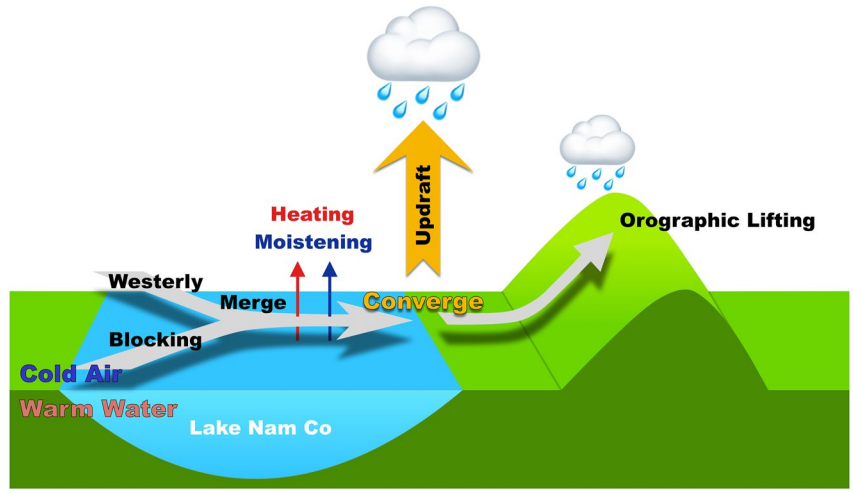

Figure 10. Schematic diagram of the influence mechanisms of the extreme snowfall event on 24 October 2006. Gray arrows denote wind field in the lower layer and yellow arrow indicates updraft and convection. Red and blue arrows denote heat and moisture transport from the lake surface to the overlying air. Rain clouds indicate precipitation centers and the sizes of them represent the intensities.

Overall, the low-level instability induced by the hydrothermal effect of LNC and topographic uplifting triggered by the dynamic effect of east NQTL dominate the extreme snowstorm that occurred sequentially over the lake and the slope of east NQTL. The dry and cold subsidence anomalies resulting from either the removal of LNC or the absence of surrounding orography (Figure 9) are not conducive to the formation of precipitation (Figures 5d–5f). Meanwhile, surface wind speed differences over the lake shore areas by lake-land friction contrast (Figures 9a and 9c) may be an additional reason for the air convergence over downwind land (X. Yao et al., 2021).

4. Summary and Discussion

In this study, the influence of LNC and surrounding orography on the extreme snowstorm on 24 October 2006 was investigated using the WRF model. From the observed data, under the large-scale environmental conditions featured by a low vortex system and westerly winds, more than 25 mm of accumulated precipitation was produced over eastern LNC and downstream area. The assessment of the control experiment showed that the simulation reasonably captured the quantitative and spatial distribution characteristics of this extreme snowstorm. By comparing the results from three sensitivity experiments with the control experiment, we revealed the respective contribution of LNC and surrounding topography and their combined contribution to the extreme snowstorm.

The main physical processes affecting this extreme snowfall event over Nam Co basin include: low-level instability caused by high lake-atmosphere temperature difference; westerly winds over the lake surface dominated by a combination of large-scale background circulation and mountain winds from west NQTL; low-level wind field blocked and deflected by the southwest-northeast trend of the mountain range; lake-effect convective snowfall triggered by water vapor convergent upward motion over the southeast lake shore; and precipitation enhancement on the slope of east NQTL by the orographic lifting in downstream of the lake (Figure 10).

Sensitive experiments suggest that the formation of extreme snowfall over Nam Co basin is determined by the combined effects of the LNC and surrounding topography, with the lake-induced thermodynamic effect being the dominant factor and the orographic dynamic effect being secondary. LNC releases a large amount of latent and sensible heat fluxes and further forms convective instability, which favors to trigger convective snowstorm. While the surrounding topography adjusts the intensity and extent of precipitation on the basic pattern of lake-induced snowfall. The upstream topography of the subsidence zone strengthens the wind field over LNC before the onset of snowfall, and the downstream topography lifts the moistened air to create an extra precipitation center. Meanwhile, the dynamic effect of lake such as lake-land roughness contrast and the thermodynamic effect of orography such as valley wind circulation are also factors influencing the precipitation distributions.

In addition, the interaction of lake and orography is not a simple linear summation but a coupled structure affecting the mesoscale circulation and transport of water vapor. Interestingly, it cannot completely suppress the formation of snowfall (reduced by 68%, see Table 1 and Figure 5c) when both LNC and the surrounding topography were removed, and the reason for which may be related to large-scale advection and transport.

The orographic effect in Nam Co basin is not consistent with the previous study. Umek and Gohm (2016) suggested that additional downstream topographic lifting is still required to trigger convection when the lake meets thermal conditions. The small size of Lake Constance (~540 km^2) and the fact that lake surface temperature during the blizzard is only 5°C higher than 2 m temperature (9°C for LNC), making the downstream topography particularly important in this event. However, the hydrothermal conditions of LNC with an area ~2,000 km^2 in this study are more adequate than those of Lake Constance, therefore harsh lifting conditions are not necessary required. Part of the released energy near the lake shore triggers convection, followed by a second uplift in the downstream orography such that the two precipitation centers are produced.

The climatic analysis identifies the area with a large precipitation amount on the downstream topography of LNC (east NQTL) in autumn (J. Xu et al., 2018). Based on the results mentioned above, it can be speculated that this is closely related to a long-term forcing caused by the westerly winds on TP and the funnel-like morphology of the Nam Co basin, which was proven by air trajectory analysis (figure not show). Numerous studies have referred to the contribution of large-scale conditions to lake-effect extreme precipitation (Alcott & Steenburgh, 2013; Shestakova & Toropov, 2021). However, few studies have focused on primary synoptic backgrounds during extreme events over lakes and surrounding areas on TP (Suriano & Leathers, 2017a, 2017b). This case study can recognize the effects of the lake and surrounding orography on extreme precipitation events to some extent, but advanced studies on climatology time scale are necessary for the generalizability of the conclusions. Revealing the roles and influence mechanisms of the lakes and complex topography in the central TP under different synoptic patterns in extreme precipitation events (Tang et al., 2021) is beneficial to further improve the refined forecasting of the extreme precipitation/snow over lake rich areas on TP.

Data Availability Statement

The authors thank Dr. Junbo Wang and Dr. Lei Huang for providing us the observation data of LNC. The authors are grateful to NASA for providing the MODIS land surface temperature product (MOD11; available at https://modis.gsfc.nasa.gov/data/dataprod/mod11.php) and the Institute of Tibetan Plateau Research, Chinese Academy of Sciences (ITPCAS) for providing the CMFD set and the meteorological observation data from the integrated observation and research station of multiple spheres in Nam Co basin (both available at https://data.tpdc.ac.cn/en/). The fifth-generation ECMWF atmospheric reanalysis (ERA5) are available online (https://www.ecmwf.int/en/forecasts/datasets/search/ERA5). The IGBP modified MODIS land-use categories and the global lake database version 2 (GLDBv2) are available at https://lpdaac.usgs.gov/products/mcd12q1v006/ and http://www.flake.igb-berlin.de/site/external-dataset, respectively.

Acknowledgments
This study is supported by National Natural Science Foundation of China under Grants 41975081, 41975130, and the National Key R&D Program of China under Grant 2017YFA0604301, CAS "Light of West China" Program (E12903010, Y929641001), the Jiangsu University "Blue Project" outstanding young teachers training object, and the Fundamental Research Funds for the Central Universities and the Jiangsu Collaborative Innovation Center for Climate Change.

References

Alcott, T. I., & Steenburgh, W. J. (2013). Orographic influences on a Great Salt Lake–Effect snowstorm. *Monthly Weather Review*, *141*(7), 2432–2450. https://doi.org/10.1175/MWR-D-12-00328.1

Behravesh, M., Mirzaei, M., & Mohebalhojeh, A. R. (2021). Comparison of mechanical and thermal effects of Lake Urmia: A case study. *Meteorology and Atmospheric Physics*, *133*(1), 109–122. https://doi.org/10.1007/s00703-020-00742-5

Biermann, T., Babel, W., Ma, W., Chen, X., Thiem, E., Ma, Y., & Foken, T. (2013). Turbulent flux observations and modelling over a shallow lake and a wet grassland in the Nam Co basin, Tibetan Plateau. *Theoretical and Applied Climatology*, *116*(1–2), 301–316. https://doi.org/10.1007/s00704-013-0953-6

Bonan, G. B. (1995). Sensitivity of a GCM simulation to inclusion of inland water surfaces. *Journal of Climate*, *8*(11), 2691–2704. https://doi.org/10.1175/1520-0442(1995)008<2691:SOAGST>2.0.CO;2

Campbell, L. S., & Steenburgh, W. J. (2017). The OWLeS IOP2b lake-effect snowstorm: Mechanisms contributing to the Tug Hill precipitation maximum. *Monthly Weather Review*, *145*(7), 2461–2478. https://doi.org/10.1175/MWR-D-16-0461.1

Choulga, M., Kourzeneva, E., Zakharova, E., & Doganovsky, A. (2014). Estimation of the mean depth of boreal lakes for use in numerical weather prediction and climate modelling. *Tellus A: Dynamic Meteorology and Oceanography*, *66*(1), 21295. https://doi.org/10.3402/tellusa.v66.21295

Cui, P., & Jia, Y. (2015). Mountain hazards in the Tibetan Plateau: Research status and prospects. *National Science Review*, *2*(4), 397–399. https://doi.org/10.1093/nsr/nwv061

Dai, Y., Chen, D., Yao, T., & Wang, L. (2020). Large lakes over the Tibetan Plateau may boost snow downwind: Implications for snow disaster. *Science Bulletin*, *65*(20), 1713–1717. https://doi.org/10.1016/j.scib.2020.06.012

Dai, Y., Wang, L., Yao, T., Li, X., Zhu, L., & Zhang, X. (2018). Observed and simulated lake effect precipitation over the Tibetan Plateau: An initial study at Nam Co Lake. *Journal of Geophysical Research: Atmospheres*, *123*(13), 6746–6759. https://doi.org/10.1029/2018JD028330

Dai, Y., Yao, T., Li, X., & Ping, F. (2018). The impact of lake effects on the temporal and spatial distribution of precipitation in the Nam Co basin, Tibetan Plateau. *Quaternary International*, *475*, 63–69. https://doi.org/10.1016/j.quaint.2016.01.075

Dai, Y., Yao, T., Wang, L., Li, X., & Zhang, X. (2020). Contrasting roles of a large alpine lake on Tibetan Plateau in shaping regional precipitation during summer and autumn. *Frontiers of Earth Science*, *8*. https://doi.org/10.3389/feart.2020.00358

Diallo, I., Giorgi, F., & Stordal, F. (2018). Influence of Lake Malawi on regional climate from a double-nested regional climate model experiment. *Climate Dynamics*, *50*(9), 3397–3411. https://doi.org/10.1007/s00382-017-3811-x

Dong, S., Peng, F., You, Q., Guo, J., & Xue, X. (2018). Lake dynamics and its relationship to climate change on the Tibetan Plateau over the last four decades. *Regional Environmental Change*, *18*(2), 477–487. https://doi.org/10.1007/s10113-017-1211-8

Du, J., Wen, L., & Su, D. (2020). Analysis of simulated temperature difference between lake surface and air and energy balance of three alpine lakes with different depths on the Qinghai-Xizang Plateau during the ice-free period. *Plateau Meteorology*, *39*(6), 1181–1194.

Dudhia, J. (1989). Numerical study of convection observed during the winter monsoon experiment using a mesoscale two-dimensional model. *Journal of the Atmospheric Sciences*, *46*(20), 3077–3107. https://doi.org/10.1175/1520-0469(1989)046<3077:NSOCOD>2.0.CO;2

Dutra, E., Stepanenko, V. M., Balsamo, G., Viterbo, P., Miranda, P. M. A., Mironov, D., & Schär, C. (2010). *An offline study of the impact of lakes on the performance of the ECMWF surface scheme* (Vol. 15, p. 13).

Eichenlaub, V. L. (1970). Lake effect snowfall to the lee of the Great Lakes: Its role in Michigan. *Bulletin of the American Meteorological Society*, *51*(5), 403–413. https://doi.org/10.1175/1520-0477(1970)051<0403:LESTTL>2.0.CO;2

Fang, N., Yang, K., Lazhu, Chen, Y., Wang, J., & Zhu, L. (2017). Research on the application of WRF-Lake modeling at Nam Co Lake on the Qinghai-Tibetan Plateau. *Plateau Meteorology*, *36*(03), 610–618.

Friedl, M. A., Sulla-Menashe, D., Tan, B., Schneider, A., Ramankutty, N., Sibley, A., & Huang, X. (2010). MODIS Collection 5 global land cover: Algorithm refinements and characterization of new datasets. *Remote Sensing of Environment*, *114*(1), 168–182. https://doi.org/10.1016/j.rse.2009.08.016

Gao, Y., Xiao, L., Chen, D., Xu, J., & Zhang, H. (2018). Comparison between past and future extreme precipitations simulated by global and regional climate models over the Tibetan Plateau. *International Journal of Climatology*, *38*(3), 1285–1297. https://doi.org/10.1002/joc.5243

Gat, J. R., & Matsui, E. (1991). Atmospheric water balance in the Amazon Basin: An isotopic evapotranspiration model. *Journal of Geophysical Research*, *96*(D7), 13179–13188. https://doi.org/10.1029/91JD00054

Ge, G., Shi, Z., Yang, X., Hao, Y., Guo, H., Kossi, F., et al. (2017). Analysis of precipitation extremes in the Qinghai-Tibetan Plateau, China: Spatio-temporal characteristics and topography effects. *Atmosphere*, *8*(7), 127. https://doi.org/10.3390/atmos8070127

Gerken, T., Biermann, T., Babel, W., Herzog, M., Ma, Y., Foken, T., & Graf, H.-F. (2013). A modelling investigation into lake-breeze development and convection triggering in the Nam Co Lake basin, Tibetan Plateau. *Theoretical and Applied Climatology*, *117*(1), 149–167. https://doi.org/10.1007/s00704-013-0987-9

Gou, P., Ye, Q., Che, T., Feng, Q., Ding, B., Lin, C., & Zong, J. (2017). Lake ice phenology of Nam Co, Central Tibetan Plateau, China, derived from multiple MODIS data products. *Journal of Great Lakes Research*, *43*(6), 989–998. https://doi.org/10.1016/j.jglr.2017.08.011

Grell, G. A., & Dévényi, D. (2002). A generalized approach to parameterizing convection combining ensemble and data assimilation techniques. *Geophysical Research Letters*, *29*(14), 38-1–38-4. https://doi.org/10.1029/2002GL015311

Gu, H., Jin, J., Wu, Y., Ek, M. B., & Subin, Z. M. (2015). Calibration and validation of lake surface temperature simulations with the coupled WRF-Lake model. *Climatic Change*, *129*(3), 471–483. https://doi.org/10.1007/s10584-013-0978-y

Gu, H., Ma, Z., & Li, M. (2016). Effect of a large and very shallow lake on local summer precipitation over the Lake Taihu basin in China. *Journal of Geophysical Research: Atmospheres*, *121*(15), 8832–8848. https://doi.org/10.1002/2015JD024098

He, J., Yang, K., Tang, W., Lu, H., Qin, J., Chen, Y., & Li, X. (2020). The first high-resolution meteorological forcing dataset for land process studies over China. *Scientific Data*, *7*(1), 25. https://doi.org/10.1038/s41597-020-0369-y

Hersbach, H., Bell, B., Berrisford, P., Hirahara, S., Horányi, A., Muñoz-Sabater, J., et al. (2020). The ERA5 global reanalysis. *Quarterly Journal of the Royal Meteorological Society*, *146*(730), 1999–2049. https://doi.org/10.1002/qj.3803

Hjelmfelt, M. R. (1992). Orographic effects in simulated lake-effect snowstorms over Lake Michigan. *Monthly Weather Review*, *120*(2), 373–377. https://doi.org/10.1175/1520-0493(1992)120<0373:OEISLE>2.0.CO;2

Hong, S.-Y., & Lim, J.-O. J. (2006). The WRF single-moment 6-class microphysics scheme (WSM6). *Asia-Pacific Journal of Atmospheric Sciences*, *42*(2), 129–151.

Hong, S.-Y., Noh, Y., & Dudhia, J. (2006). A new vertical diffusion package with an explicit treatment of entrainment processes. *Monthly Weather Review*, *134*(9), 2318–2341. https://doi.org/10.1175/MWR3199.1

Huang, A., Lazhu, Wang, J., Dai, Y., Yang, K., Wei, N., et al. (2019). Evaluating and improving the Performance of three 1-D Lake models in a large deep Lake of the central Tibetan Plateau. *Journal of Geophysical Research: Atmospheres*, *124*(6), 3143–3167. https://doi.org/10.1029/2018JD029610

Ji, Q., Yang, T., Dong, J., & He, Y. (2018). Glacier variations in response to climate change in the eastern Nyainqêntanglha Range, Tibetan Plateau from 1999 to 2015. *Arctic Antarctic and Alpine Research*, *50*(1), e1435844. https://doi.org/10.1080/15230430.2018.1435844

Koseki, S., & Mooney, P. A. (2019). Influences of Lake Malawi on the spatial and diurnal variability of local precipitation. *Hydrology and Earth System Sciences*, *23*(7), 2795–2812. https://doi.org/10.5194/hess-23-2795-2019

Kourzeneva, E. (2010). External data for lake parameterization in Numerical Weather Prediction and climate modeling. *External Data for Lake Parameterization in Numerical Weather Prediction and Climate Modeling*, *15*(2), 165–177.

Kristovich, D. A. R., Laird, N. F., & Hjelmfelt, M. R. (2003). Convective evolution across Lake Michigan during a widespread lake-effect snow event. *Monthly Weather Review*, *131*(4), 643–655. https://doi.org/10.1175/1520-0493(2003)131<0643:CEALMD>2.0.CO;2

Kristovich, D. A. R., & Spinar, M. L. (2005). Diurnal variations in lake-effect precipitation near the western Great Lakes. *Journal of Hydrometeorology*, *6*(2), 210–218. https://doi.org/10.1175/JHM403.1

Kropacek, J., Feng, C., Alle, M., Kang, S., & Hochschild, V. (2010). Temporal and spatial aspects of snow distribution in the Nam Co basin on the Tibetan Plateau from MODIS data. *Remote Sensing*, *2*(12), 2700–2712. https://doi.org/10.3390/rs2122700

Lang, C. E., McDonald, J. M., Gaudet, L. C., Doeblin, D., Jones, E. A., & Laird, N. F. (2018). *The influence of a lake-to-lake connection from Lake Huron on the lake-effect snowfall in the vicinity of Lake Ontario*. https://doi.org/10.1175/JAMC-D-17-0225.1

Lazhu, Yang, K., Wang, J., Lei, Y., Chen, Y., Zhu, L., & Qin, J. (2016). Quantifying evaporation and its decadal change for Lake Nam Co, central Tibetan Plateau. *Journal of Geophysical Research: Atmospheres*, *121*(13), 7578–7591. https://doi.org/10.1002/2015JD024523

Li, M., Ma, Y., Hu, Z., Ishikawa, H., & Oku, Y. (2009). Snow distribution over the Namco lake area of the Tibetan Plateau. *Hydrology and Earth System Sciences*, *13*(11), 2023–2030. https://doi.org/10.5194/hess-13-2023-2009

López-Espinoza, E., Ruiz-Angulo, A., Zavala-Hidalgo, J., Romero-Centeno, R., & Escamilla-Salazar, J. (2019). Impacts of the desiccated Lake system on Precipitation in the basin of Mexico City. *Atmosphere*, *10*(10), 628. https://doi.org/10.3390/atmos10100628

Ma, Y., Lu, M., Chen, H., Pan, M., & Hong, Y. (2018). Atmospheric moisture transport versus precipitation across the Tibetan Plateau: A mini-review and current challenges. *Atmospheric Research*, *209*, 50–58. https://doi.org/10.1016/j.atmosres.2018.03.015

Ma, Y., Wang, Y., Wu, R., Hu, Z., Yang, K., Li, M., et al. (2009). Recent advances on the study of atmosphere-land interaction observations on the Tibetan Plateau. *Hydrology and Earth System Sciences*, *13*(7), 1103–1111. https://doi.org/10.5194/hess-13-1103-2009

Ma, Y., Yang, Y., Qiu, C., & Wang, C. (2019). Evaluation of the WRF-Lake model over two major freshwater lakes in China. *Journal of Meteorological Research*, *33*(2), 219–235. https://doi.org/10.1007/s13351-019-8070-9

MacKay, M. D., Neale, P. J., Arp, C. D., De Senerpont Domis, L. N., Fang, X., Gal, G., et al. (2009). Modeling lakes and reservoirs in the climate system. *Limnology & Oceanography*, *54*(6part2), 2315–2329. https://doi.org/10.4319/lo.2009.54.6_part_2.2315

Mallard, M. S., Nolte, C. G., Bullock, O. R., Spero, T. L., & Gula, J. (2014). Using a coupled lake model with WRF for dynamical downscaling. *Journal of Geophysical Research: Atmospheres*, *119*(12), 7193–7208. https://doi.org/10.1002/2014JD021785

Mallard, M. S., Nolte, C. G., Spero, T. L., Bullock, O. R., Alapaty, K., Herwehe, J. A., et al. (2015). Technical challenges and solutions in representing lakes when using WRF in downscaling applications. *Geoscientific Model Development*, *8*(4), 1085–1096. https://doi.org/10.5194/gmd-8-1085-2015

Maussion, F., Scherer, D., Finkelnburg, R., Richters, J., Yang, W., & Yao, T. (2010). *WRF simulation of a precipitation event over the Tibetan Plateau, China – An assessment using remote sensing and ground observations (preprint). Hydrometeorology/Modelling approaches*. Retrieved from https://hess.copernicus.org/preprints/7/3551/2010/hessd-7-3551-2010.pdf

Miner, T. J., & Fritsch, J. M. (1997). Lake-effect rain events. *Monthly Weather Review*, *125*(12), 3231–3248. https://doi.org/10.1175/1520-0493(1997)125<3231:LERE>2.0.CO;2

Mlawer, E. J., Taubman, S. J., Brown, P. D., Iacono, M. J., & Clough, S. A. (1997). Radiative transfer for inhomogeneous atmospheres: RRTM, a validated correlated-k model for the longwave. *Journal of Geophysical Research*, *102*(D14), 16663–16682. https://doi.org/10.1029/97JD00237

Nicholson, S. E., & Yin, X. (2002). Mesoscale patterns of rainfall, cloudiness and evaporation over the Great Lakes of East Africa. In E. O. Odada & D. O. Olago (Eds.), *The East African Great Lakes: Limnology, Palaeolimnology and Biodiversity* (pp. 93–119). Springer Netherlands. https://doi.org/10.1007/0-306-48201-0_3

Niziol, T. A., Snyder, W. R., & Waldstreicher, J. S. (1995). Winter weather forecasting throughout the eastern United States. Part IV: Lake effect snow. *Weather and Forecasting*, *10*(1), 61–77. https://doi.org/10.1175/1520-0434(1995)010<0061:WWFTTE>2.0.CO;2

Notaro, M., Holman, K., Zarrin, A., Fluck, E., Vavrus, S., & Bennington, V. (2013). Influence of the Laurentian Great Lakes on regional climate. *Journal of Climate*, *26*(3), 789–804. https://doi.org/10.1175/jcli-d-12-00140.1

Notaro, M., Zarrin, A., Vavrus, S., & Bennington, V. (2013). Simulation of heavy lake-effect snowstorms across the Great Lakes basin by RegCM4: Synoptic climatology and variability. *Monthly Weather Review*, *141*(6), 1990–2014. https://doi.org/10.1175/MWR-D-11-00369.1

Onton, D. J., & Steenburgh, W. J. (2001). Diagnostic and sensitivity studies of the 7 December 1998 Great Salt Lake–Effect snowstorm. *Monthly Weather Review*, *129*(6), 1318–1338. https://doi.org/10.1175/1520-0493(2001)129<1318:DASSOT>2.0.CO;2

Powers, J. G., Klemp, J. B., Skamarock, W. C., Davis, C. A., Dudhia, J., Gill, D. O., et al. (2017). The weather research and forecasting model: Overview, system efforts, and future directions. *Bulletin of the American Meteorological Society*, *98*(8), 1717–1737. https://doi.org/10.1175/BAMS-D-15-00308.1

Samuelsson, P., Kourzeneva, E., & Mironovm, D. (2010). The impact of lakes on the European climate as simulated by a regional climate model. *Boreal Environment Research*, *15*(2), 113–129.

Scott, R. W., & Huff, F. A. (1996). Impacts of the Great Lakes on regional climate conditions. *Journal of Great Lakes Research*, *22*(4), 845–863. https://doi.org/10.1016/S0380-1330(96)71006-7

Shestakova, A. A., & Toropov, P. A. (2021). Orographic and lake effect on extreme precipitation on the Iranian coast of the Caspian sea: A case study. *Meteorology and Atmospheric Physics*, *133*(1), 69–84. https://doi.org/10.1007/s00703-020-00735-4

Shi, Q., & Xue, P. (2019). Impact of lake surface temperature variations on lake effect snow over the Great Lakes region. *Journal of Geophysical Research: Atmospheres*, *124*(23), 12553–12567. https://doi.org/10.1029/2019JD031261

Su, D., Wen, L., Gao, X., Lepparanta, M., Song, X., Shi, Q., & Kirillin, G. (2020). Effects of the largest lake of the Tibetan Plateau on the regional climate. *Journal of Geophysical Research: Atmospheres*, *125*(22), e2020JD033396. https://doi.org/10.1029/2020JD033396

Su, D., Wen, L., Zhao, L., Li, Z., & Du, J. (2019). Numerical simulation of seasonal local climate effect in Qinghai Lake. *Plateau Meteorology*, *38*(5), 944–958.

Subin, Z. M., Riley, W. J., & Mironov, D. (2012). An improved lake model for climate simulations: Model structure, evaluation, and sensitivity analyses in CESM1. *Journal of Advances in Modeling Earth Systems*, *4*(1). https://doi.org/10.1029/2011MS000072

Sun, F., Ma, R., He, B., Zhao, X., Zeng, Y., Zhang, S., & Tang, S. (2020). Changing patterns of lakes on the southern Tibetan Plateau based on multi-source satellite data. *Remote Sensing*, *12*(20), 3450. https://doi.org/10.3390/rs12203450

Sun, J., Yang, K., Guo, W., Wang, Y., He, J., & Lu, H. (2020). Why has the inner Tibetan Plateau become wetter since the mid-1990s? *Journal of Climate*, *33*(19), 8507–8522. https://doi.org/10.1175/JCLI-D-19-0471.1

Suriano, Z. J., & Leathers, D. J. (2017a). Synoptic climatology of lake-effect snowfall conditions in the eastern Great Lakes region. *International Journal of Climatology*, *37*(12), 4377–4389. https://doi.org/10.1002/joc.5093

Suriano, Z. J., & Leathers, D. J. (2017b). Synoptically classified lake-effect snowfall trends to the lee of Lakes Erie and Ontario. *Climate Research*, *74*(1), 1–13. https://doi.org/10.3354/cr01480

Tang, Y., Huang, A., Wu, P., Huang, D., Xue, D., & Wu, Y. (2021). Drivers of summer extreme precipitation events over East China. *Geophysical Research Letters*, *48*(11), e2021GL093670. https://doi.org/10.1029/2021GL093670

Tewari, M., Chen, F., Wang, W., Dudhia, J., LeMone, M. A., Gayno, G., et al. (2004). *14.2A Implementation and verification of the unified Noah land surface model in the WRF model* (Vol. 6).

Thiery, W., Davin, E. L., Seneviratne, S. I., Bedka, K., Lhermitte, S., & van Lipzig, N. P. M. (2016). Hazardous thunderstorm intensification over Lake Victoria. *Nature Communications*, *7*(1), 12786. https://doi.org/10.1038/ncomms12786

Umek, L., & Gohm, A. (2016). Lake and orographic effects on a snowstorm at Lake Constance. *Monthly Weather Review*, *144*(12), 4687–4707. https://doi.org/10.1175/MWR-D-16-0032.1

Van de Walle, J., Thiery, W., Brousse, O., Souverijns, N., Demuzere, M., & van Lipzig, N. P. M. (2020). A convection-permitting model for the Lake Victoria basin: Evaluation and insight into the mesoscale versus synoptic atmospheric dynamics. *Climate Dynamics*, *54*(3), 1779–1799. https://doi.org/10.1007/s00382-019-05088-2

Veals, P. G., Steenburgh, W. J., & Campbell, L. S. (2018). Factors affecting the inland and orographic enhancement of lake-effect precipitation over the Tug Hill Plateau. *Monthly Weather Review*, *146*(6), 1745–1762. https://doi.org/10.1175/MWR-D-17-0385.1

Wan, W., Xiao, P., Feng, X., Li, H., Ma, R., Duan, H., & Zhao, L. (2014). Monitoring lake changes of Qinghai-Tibetan Plateau over the past 30 years using satellite remote sensing data. *Chinese Science Bulletin*, *59*(8), 701–714. https://doi.org/10.1007/s11434-014-0128-6

Wang, B., Ma, Y., Chen, X., Ma, W., Su, Z., & Menenti, M. (2015). Observation and simulation of lake-air heat and water transfer processes in a high-altitude shallow lake on the Tibetan Plateau. *Journal of Geophysical Research: Atmospheres*, *120*(24), 12327–12344. https://doi.org/10.1002/2015JD023863

Wang, B., Ma, Y., Su, B., Wang, Y., & Ma, W. (2020). Quantifying the evaporation amounts of 75 high-elevation large dimictic lakes on the Tibetan Plateau. *Science Advances*, *6*(26), eaay8558. https://doi.org/10.1126/sciadv.aay8558

Wang, F., Ni, G., Riley, W. J., Tang, J., Zhu, D., & Sun, T. (2019). Evaluation of the WRF lake module (v1.0) and its improvements at a deep reservoir. *Geoscientific Model Development*, *12*(5), 2119–2138. https://doi.org/10.5194/gmd-12-2119-2019

Wang, J., Zhu, L., Daut, G., Ju, J., Lin, X., Wang, Y., & Zhen, X. (2009). Investigation of bathymetry and water quality of Lake Nam Co, the largest lake on the central Tibetan Plateau, China. *Limnology*, *10*(2), 149–158. https://doi.org/10.1007/s10201-009-0266-8

Wang, L., Zeng, Y., & Zhong, L. (2017). Impact of climate change on tourism on the Qinghai-Tibetan Plateau: Research based on a literature review. *Sustainability*, *9*(9), 1539. https://doi.org/10.3390/su9091539

Wang, Y., & Wu, G. (2018). *Meteorological observation data from the integrated observation and research station of multiple spheres in Namco (2005–2016)*. National Tibetan Plateau Data Center. https://doi.org/10.11888/AtmosPhys.tpe.00000049.file

Wen, L., Lv, S., Li, Z., Zhao, L., & Nagabhatla, N. (2015). Impacts of the two biggest lakes on local temperature and precipitation in the Yellow River source region of the Tibetan Plateau. *Advances in Meteorology*, *2015*, e248031. https://doi.org/10.1155/2015/248031

Wen, L., Lyu, S., Kirillin, G., Li, Z., & Zhao, L. (2016). Air–lake boundary layer and performance of a simple lake parameterization scheme over the Tibetan highlands. *Tellus A: Dynamic Meteorology and Oceanography*, *68*(1), 31091. https://doi.org/10.3402/tellusa.v68.31091

Wonsick, M. M., & Pinker, R. T. (2014). The radiative environment of the Tibetan Plateau. *International Journal of Climatology*, *34*(7), 2153–2162. https://doi.org/10.1002/joc.3824

Wu, Y., Huang, A., Lazhu, Yang, X., Qiu, B., Wen, L., et al. (2020). Improvements of the coupled WRF-Lake model over Lake Nam Co, central Tibetan Plateau. *Climate Dynamics*, *55*(9–10), 2703–2724. https://doi.org/10.1007/s00382-020-05402-3

Wu, Y., Huang, A., Yang, B., Dong, G., Wen, L., Lazhu, et al. (2019). Numerical study on the climatic effect of the lake clusters over Tibetan Plateau in summer. *Climate Dynamics*, *53*(9–10), 5215–5236. https://doi.org/10.1007/s00382-019-04856-4

Wu, Y., & Zhu, L. (2008). The response of lake-glacier variations to climate change in Nam Co Catchment, central Tibetan Plateau, during 1970–2000. *Journal of Geographical Sciences*, *18*(2), 177–189. https://doi.org/10.1007/s11442-008-0177-3

Xiao, C., Lofgren, B. M., & Wang, J. (2018). WRF-based assessment of the Great Lakes' impact on cold season synoptic cyclones. *Atmospheric Research*, *214*, 189–203. https://doi.org/10.1016/j.atmosres.2018.07.020

Xiao, C., Lofgren, B. M., Wang, J., & Chu, P. Y. (2016). Improving the lake scheme within a coupled WRF-lake model in the Laurentian Great Lakes. *Journal of Advances in Modeling Earth Systems*, *8*(4), 1969–1985. https://doi.org/10.1002/2016MS000717

Xu, J., Ma, Y., Sun, F., & Ma, W. (2018). Analysis of effects of lake and upstream orography on the precipitation in fall over Nam Co area. *Plateau Meteorology*, *37*(6), 1535–1543.

Xu, L., & Liu, H. (2015). Numerical simulation of the lake effect of Erhai in the Yunnan-Guizhou Plateau area. *Acta Meteorologica Sinica*, *73*(04), 789–802.

Xu, L., Liu, H., & Cao, J. (2014). Numerical simulation of local circulation over the Cangshan Mountain−Erhai Lake area in Dali, Southwest China. *Chinese Journal of Atmospheric Sciences*, *38*(6), 1198–1210.

Xu, L., Liu, H., Du, Q., & Wang, L. (2016). Evaluation of the WRF-Lake model over a highland freshwater lake in southwest China. *Journal of Geophysical Research: Atmospheres*, *121*(23), 13989–14005. https://doi.org/10.1002/2016JD025396

Xu, Y., Kang, S., Zhang, Y., & Zhang, Y. (2011). A method for estimating the contribution of evaporative vapor from the Lake Nam Co to local atmospheric vapor based on stable isotopes of water bodies. *Chinese Science Bulletin*, *56*(13), 1042–1049. https://doi.org/10.1007/s11434-011-4467-2

Yang, K., & He, J. (2019). *China meteorological forcing dataset (1979–2018)*. National Tibetan Plateau Data Center. https://doi.org/10.11888/AtmosphericPhysics.tpe.249369.file

Yang, X., Lü, Y., Ma, Y., & Wen, J. (2015). Summertime thermally-induced circulations over the Lake Nam Co region of the Tibetan Plateau. *Journal of Meteorological Research*, *29*(2), 305–314. https://doi.org/10.1007/s13351-015-4024-z

Yang, X., Lü, Y., Wen, J., Ma, Y., Meng, X., Huang, A., et al. (2021). Numerical simulation of typical characteristics of land surface water-heat exchange over Gyaring Lake and Ngoring Lake in summer. *Plateau Meteorology*, 1–10.

Yao, T., Masson-Delmotte, V., Gao, J., Yu, W., Yang, X., Risi, C., et al. (2013). A review of climatic controls on $\delta^{18}O$ in precipitation over the Tibetan Plateau: Observations and simulations. *Reviews of Geophysics*, *51*(4), 525–548. https://doi.org/10.1002/rog.20023

Yao, X., Yang, K., Zhou, X., Wang, Y., Lazhu, Chen, Y., & Lu, H. (2021). Surface friction contrast between water body and land enhances precipitation downwind of a large lake in Tibet. *Climate Dynamics*, *56*(7–8), 2113–2126. https://doi.org/10.1007/s00382-020-05575-x

Zhang, G., Bolch, T., Chen, W., & Crétaux, J.-F. (2021). Comprehensive estimation of lake volume changes on the Tibetan Plateau during 1976–2019 and basin-wide glacier contribution. *Science of the Total Environment*, *772*, 145463. https://doi.org/10.1016/j.scitotenv.2021.145463

Zhang, X., Duan, K., Shi, P., & Yang, J. (2016). Effect of lake surface temperature on the summer precipitation over the Tibetan Plateau. *Journal of Mountain Science*, *13*(5), 802–810. https://doi.org/10.1007/s11629-015-3743-z

Zhu, L., Jin, J., Liu, X., Tian, L., & Zhang, Q. (2018). Simulations of the impact of lakes on local and regional climate over the Tibetan Plateau. *Atmosphere-Ocean*, *56*(4), 230–239. https://doi.org/10.1080/07055900.2017.1401524

Zhu, L., Jin, J., & Liu, Y. (2020). Modeling the effects of lakes in the Tibetan Plateau on diurnal variations of regional climate and their seasonality. *Journal of Hydrometeorology*, *21*(11), 2523–2536. https://doi.org/10.1175/JHM-D-20-0091.1

Zhu, L., Zhang, G., Yang, R., Liu, C., Yang, K., Qiao, B., & Han, B. (2019). Lake variations on Tibetan Plateau of recent 40 years and future changing tendency. *Bulletin of Chinese Academy of Sciences*, *34*(11), 1254–1263.